Influence of sinusoidal motion on Stirling engines

by

Salvatore Ranieri

A thesis submitted to the
School of Graduate and Postdoctoral Studies in partial
fulfillment of the requirements for the degree of

Master of Applied Science in Mechanical Engineering

The Faculty of Engineering and Applied Science

University of Ontario Institute of Technology

Oshawa, Ontario, Canada

December 2018

Thesis Examination Information

Submitted by: **Salvatore Ranieri**

Master of Applied Science in **Mechanical Engineering**

Thesis title: Influence of sinusoidal motion on Stirling engines

An oral defense of this thesis took place on December 11, 2018 in front of the following examining committee:

Examining Committee:

Chair of Examining Committee	Dr. Martin Agelin-Chaab
Research Supervisor	Dr. Brendan MacDonald
Examining Committee Member	Dr. Bale Reddy
External Examiner	Dr. Dipal Patel, UOIT Automotive Engineering Faculty

The above committee determined that the thesis is acceptable in form and content and that a satisfactory knowledge of the field covered by the thesis was demonstrated by the candidate during an oral examination. A signed copy of the Certificate of Approval is available from the School of Graduate and Postdoctoral Studies.

Abstract

Stirling engines have a high potential to produce renewable energy due to their ability to use a wide range of sustainable heat sources and their high theoretical efficiencies. They have not yet achieved widespread use and commercial Stirling engines have had reduced efficiencies compared to their ideal values. This work shows that a substantial amount of the reduction in efficiency is due to the operation of Stirling engines using sinusoidal motion and quantifies this reduction. A discrete model was developed to perform an isothermal analysis of a 100cc alpha-type Stirling engine with a 90° phase angle offset, to demonstrate the impact of sinusoidal motion on the net work and thermal efficiency in comparison to the ideal cycle. The model was adapted to analyze beta and gamma-type Stirling configurations, and the analysis revealed similar reductions due to sinusoidal motion. Lastly, a mechanically plausible arrangement is presented and analyzed to demonstrate that non-sinusoidal operation can be accomplished.

Keywords: Stirling engine; Efficiency; Thermodynamics; Sinusoidal

Author's Declaration

I hereby declare that this thesis consists of original work of which I have authored. This is a true copy of the thesis, including any required final revisions, as accepted by my examiners.

I authorize the University of Ontario Institute of Technology to lend this thesis to other institutions or individuals for the purpose of scholarly research. I further authorize University of Ontario Institute of Technology to reproduce this thesis by photocopying or by other means, in total or in part, at the request of other institutions or individuals for the purpose of scholarly research. I understand that my thesis will be made electronically available to the public.

Salvatore Ranieri

Abstract

Stirling engines have a high potential to produce renewable energy due to their ability to use a wide range of sustainable heat sources and their high theoretical efficiencies. They have not yet achieved widespread use and commercial Stirling engines have had reduced efficiencies compared to their ideal values. This work shows that a substantial amount of the reduction in efficiency is due to the operation of Stirling engines using sinusoidal motion and quantifies this reduction. A discrete model was developed to perform an isothermal analysis of a 100cc alpha-type Stirling engine with a 90° phase angle offset, to demonstrate the impact of sinusoidal motion on the net work and thermal efficiency in comparison to the ideal cycle. The model was adapted to analyze beta and gamma-type Stirling configurations, and the analysis revealed similar reductions due to sinusoidal motion. Lastly, a mechanically plausible arrangement is presented and analyzed to demonstrate that non-sinusoidal operation can be accomplished.

Keywords: Stirling engine; Efficiency; Thermodynamics; Sinusoidal

Statement of Contributions

Part of the work described in Chapter 3 has been published as:

S. Ranieri, G. Prado, and B. MacDonald. Efficiency reduction in stirling engines resulting from sinusoidal motion. Energies, 11(11):2887, 2018.

I performed the literature review, the majority of the analysis, and presented the findings for the above mentioned publication.

I am the sole author of section 3.6 in the results and discussion of this thesis. The creative works and/or the inventive knowledge described in this section has not been previously published.

Acknowledgements

I would like to begin by thanking a few, among many, that have helped make this project possible.

Thanks to my supervisor, Professor Brendan Macdonald, for his support, enthusiasm, and academic teachings of both thermodynamics and fluid mechanics. He is incredibly intelligent and his love for engineering is inspiring. I would like to thank my lab mates and colleagues: Henry Fung, Michael Crowley, Mostasim Mahmud, Anders Neilson, William Oishi, and Justin Rizzi for the often profound discussions and synergy. Thank you to my supervisory committee, Professor Bale Reddy and Professor Brendan MacDonald, for dedicating their time to assess my work. Also a special thanks to Professor Dipal Patel for agreeing to be the external examiner and for thorough examination of the work.

A very big thanks to my fiancée Virginia Bertucci. Her own determination and success motivates me to pursue seemingly impossible challenges, while her patience enables my passion and excitement.

Finally, I would like to thank my family for their love and support. A very special thanks to my parents Rita and Nino who encourage me at every step, provide experience, and financial support over the years. Their love is astonishing.

Contents

List of Tables

List of Figures

Nomenclature

V_H	hot volume (cm^3)
V_C	cold volume (cm^3)
V_R	regenerator volume (cm^3)
V_{total}	total volume of working fluid (cm^3)
V_{DH}	hot space dead volume (cm^3)
V_{DC}	cold space dead volume (cm^3)
m_{system}	total mass of working fluid (kg)
m_H	mass of working fluid within hot volume (kg)
m_C	mass of working fluid within cold volume (kg)
m_R	mass of working fluid within regenerator (kg)
v	specific volume (m^3/kg)
P	engine pressure (kPa)
R	gas constant (J/kg K)
T_H	hot temperature (K)
T_C	cold temperature (K)
T_R	regenerator temperature (K)
T_{global}	total average temperature (K)
s	specific entropy (J/kg K)
W_H	work from hot piston (J)
W_C	work from cold piston (J)
W_{net}	total work produced (J)
Q_{in}	heat addition (J)
Q_{out}	heat rejection (J)
y	incremental cam lift (cm)
L	cam/displacer stroke (cm)
r	cam radius (cm)

Greek letters

α	phase angle (°)
η_{th}	thermal efficiency
θ	crank angle (°)
β	cam rise or return duration (°)
ϕ	cam pressure angle (°)
Δ	discrete change

Chapter 1

Introduction

In recent years sustainability has been a global topic of importance. With an environmentally frivolous past and a seemingly incapable ability to alter current global human consumption, the earth's habitable future is seemingly unclear. A large contributing factor to the degradation of the planet is due to green house gasses, as a byproduct of energy conversion from fossil fuels. Further evidenced by accelerating climate change, global population growth, and the depletion of fossil fuels; alternate and sustainable technologies are, now more than ever, required to maintain a habitable earth. The Stirling engine is capable converting heat energy into useful work while operating on a variety of heat sources, including completely renewable sources such as the sun, making them a promising technology for the future.

The Stirling cycle has a theoretical efficiency equivalent to that of the Carnot cycle, which is the maximum possible efficiency that any engine cycle can operate at within specific temperature limits [1]. However, the promise of Stirling engines has fallen short of expectation. In practice Stirling engines do not operate to their acclaimed efficiencies,

and commercially available systems are only able to convert energy with efficiency values comparable to diesel engines [2]. The deviation from the ideal values differ beyond mechanical losses alone.

The mechanical simplicity of pistons connected to a crank shaft may be hindering the ability of the Stirling engine to follow the cycle, thus inhibiting it's maximum performance and efficiency potential. This thesis will investigate the possibility that the motion imposed by crankshafts, resulting in continuous sinusoidal motion of parts, may result in a reduction of the Stirling engine's efficiency.

1.1 Technical Background

The ideal Stirling thermodynamic cycle with a regenerator operates on four steps; isothermal compression from piston work input, isochoric heat addition from regeneration, isothermal expansion from piston work output, and isochoric heat rejection into the regenerator. The regenerator is typically a porous heat exchanger, often in the form of fine wire mesh, that has an immense ability to transfer heat due to its high surface area to volume ratio and acts as an energy storage device to increase efficiency. Commonly, the Stirling engine is a piston-reciprocation device made up of pistons connected to a crankshaft, producing sinusoidal motion of parts. Because of the disorderly engine motion the Stirling engine may be unable to adhere to the ideal thermodynamic processes, and the operational differences must be carefully detailed.

1.1.1 Ideal Stirling cycle operation

To demonstrate the working principle behind the ideal Stirling cycle it is necessary to understand a standard two piston arrangement with a regenerator fixed in between them as shown in Figure 1. For this explanation the left piston will be denoted as the compression piston which controls the cold volume, and the right piston as the expansion piston which controls the hot volume.

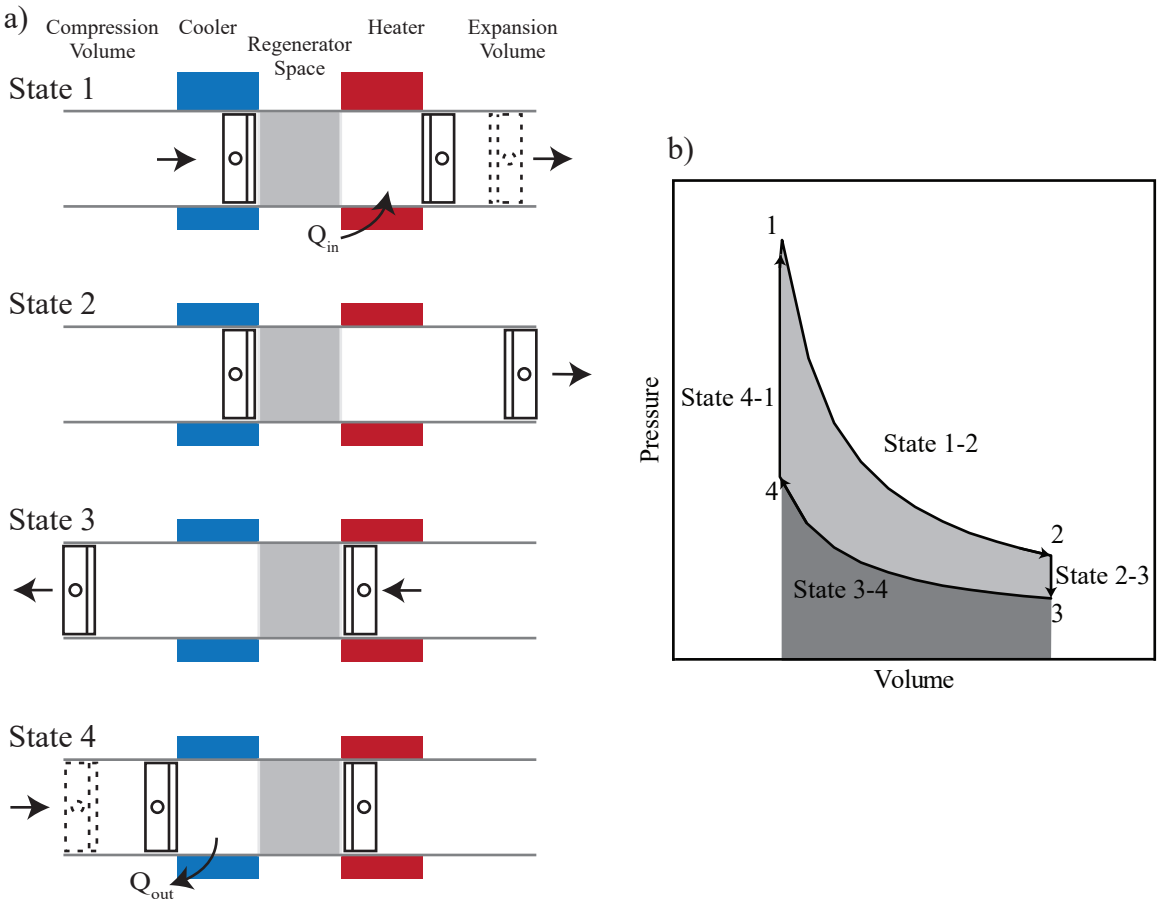

Figure 1. A generic a) schematic and b) P-V diagram for the four thermodynamic steps of an ideal Stirling cycle.

Isothermal expansion (State 1 to 2)

Isothermal expansion can be characterized as the work output state and is the step of the cycle in which useful energy is attained. During this process the expansion piston is moving outward while the compression piston remains at rest from state 1 to 2 shown in Figure 1a, expanding the overall volume of the Stirling engine to the maximum volume. It is important to note that by having the cold piston remain at rest in it's most right position constrains the fluid to be completely isolated on the hot side of the engine, enabling ideal expansion characteristics . While this piston is expanding the external heat source must compensate the working fluid by adding energy to keep the temperature constant and prevent adiabatic cooling, thereby maximizing the effectiveness of the expansion process and the net work produced. This results in the sloped line on the P-V diagram shown in Figure 1b from state 1 to 2 corresponding to the transition from the minimum to the maximum engine volume. The area under this line, shown by both the light and dark gray shaded areas in Figure 1b, equates to the work produced by this process.

Isochoric heat rejection (State 2 to 3)

Following the expansion step, both the expansion piston and the compression piston move from their respective right most to their left most position in a synchronous fashion, depicted by state 2 to 3 of Figure 1a. After this process, the expansion volume has decreased to its minimum and all of the working fluid resides in the compression volume. By moving together the pistons do not change the overall volume within the engine,

resulting in a vertical line on the P-V diagram shown in Figure 1b, thus producing no work. As the pistons force the fluid through the regenerator the hot gasses cool by the heat transfer between the working fluid and the regenerator. The now hot regenerator stores this energy for the next regeneration step.

Isothermal compression (State 3 to 4)

The next step involves charging the working fluid by compression. To do so, the compression piston moves from its left most position to its most compressed position while the expansion piston remains at rest as shown in Figure 1a from state 3 to 4. To prevent the working fluid from adiabatic heating during this process, the external heat sink compensates the working fluid by simultaneously draining the excess energy to retain a constant temperature, therefore maximizing the effectiveness of the compression process. This results in the sloped line on the P-V diagram shown in Figure 1b from state 3 to 4 corresponding to the transition from the maximum to the minimum engine volume. The area under this line, shown by the dark gray shaded area in Figure 1b, equates to the work required to produce this process and can be characterized as the work input process.

Isochoric heat addition (State 4 to 1)

Lastly, both the expansion and compression pistons move synchronously from the compression position to the beginning of the expansion position as shown in Figure 1a from state 4 to 1. By moving together the pistons do not change the overall volume within the engine, resulting in a vertical line on the P-V diagram shown in Figure 1b, thus produc-

ing no work. The working fluid is forced back through the regenerator where the initially deposited heat energy is regained. The now cold regenerator remains cold until the next cycle. At this point, the compression volume is now at its minimum and all of the energy dense working fluid resides in the expansion volume, ready for isothermal expansion to begin again. If the regeneration steps are both perfectly isochoric, the net work can be calculated as the difference between the isothermal expansion and compression processes, and is graphically represented by the light gray shaded area on the P-V diagram shown in Figure 1b.

1.1.2 Stirling engine configurations

The embodiment of the Stirling cycle takes the form of the Stirling engine, which is an approximation of the theoretical thermodynamic cycle. This is made possible with three different engine configurations, depending on the application and desired output [3]. Stirling engine configurations vary with respect to; the arrangement and locations of pistons, displacers, and regenerators, the thermal-fluid passageways; the orientations of heat-exchangers; and mechanical/ electro-mechanical drive mechanisms. Regardless of the configuration, the outcome remains the same, that is, converting heat energy into shaft energy while operating with continuous sinusoidal motion of parts. The commonly explored configurations and mechanisms are described in the following subsections.

Alpha-type

The alpha-type Stirling engine utilizes two pistons within two separate cylinders, an expansion and a compression piston, which control the hot and cold volumes respectively. The thermal passageway is between the two heads of the cylinder, and houses the regenerator [4]. Figure 2 is a schematic that represents the alpha-type Stirling engine.

This configuration utilizes a crank shaft mechanism with a single journal bearing that joins the expansion and compression pistons from the connecting rods. This arrangement produces sinusoidal piston motion with a phase angle offset, α, between the two pistons governed by the angle between the cylinders' axes.

Beta-type

The beta-type Stirling engine utilizes a piston and a displacer with both components sharing the same cylinder. In this configuration, the piston's sole purpose is to compress the cold working fluid and expand the hot working fluid. The displacer is not responsible

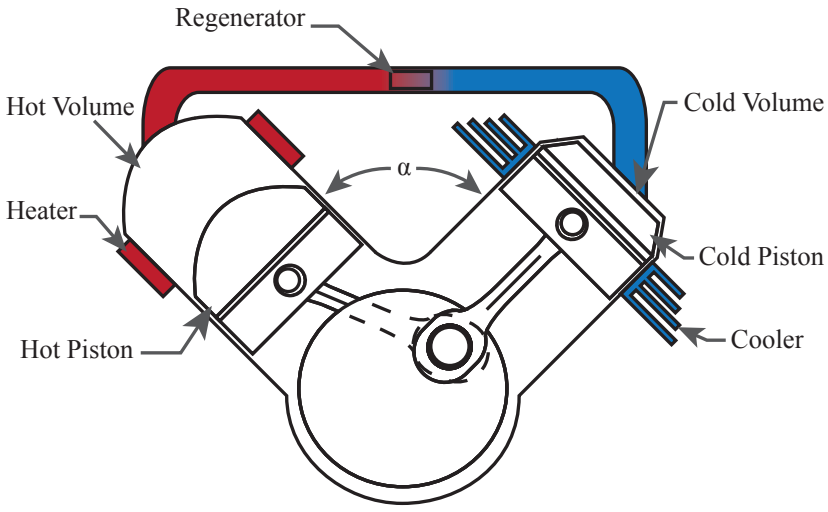

Figure 2. Schematic of an alpha-type Stirling engine.

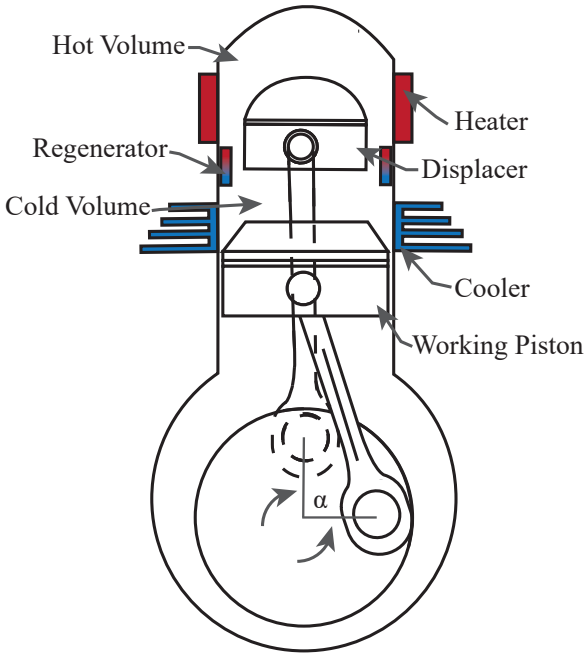

Figure 3. Schematic of an beta-type Stirling engine.

for any power transfer as it is exposed to equal pressure on all sides of its surfaces. The displacer's sole purpose is to control how much volume is on either side of the engine by residing in the opposite space [5]. Figure 3 is a schematic that represents the beta-type Stirling engine.

Figure 3 shows the working fluid contained above the power piston and occupying the void volume around the displacer. Alternatively, designers may opt to add seals to the displacer and create an external fluid path, effectively allowing for external heat exchangers. The regenerator is placed in the connection between the hot and cold working volumes. This configuration utilizes a crank shaft mechanism with two journal bearings, allowing the connecting rods of the piston and displacer to attach in separate locations. This arrangement produces sinusoidal motion with a phase angle offset, α, between the piston and displacer governed by the angle between the two journal bearings and the center axis of rotation.

Free piston

The free piston Stirling engine is identical to the beta-type Stirling engine configuration and component layout, differing only in how the piston and displacer are coupled to the drive mechanism. The free piston Stirling engine has no mechanical coupling, rather it utilizes an electro-mechanical coupling with an electrical generator to convert the kinetic energy of the piston and displacer movement directly into electric energy. This design often employs a gas spring system that effectively bounces the piston after reaching its most bottom location, resulting in sinusoidal motion of parts.

Gamma-type

The gamma-type Stirling engine utilizes a piston and a displacer, however is unique in that both the piston and displacer operate within their own cylinders. Again, the piston in solely responsible for work input and output through compression and expansion respectively, while the displacer controls the location of the working fluid. Figure 4 is a schematic that can represent the gamma-type Stirling engine.

The working fluid is contained above the power piston and around the displacer's void volume. The cylinders have a passageway between them, typically spanning from the bottom of the displacer cylinder to the top of the piston cylinder. Alternatively, designers may opt to add seals to the displacer and create an external fluid path, effectively allowing for external heat exchangers. The regenerator is placed in the connection between the two working volumes. This configuration utilizes a crank shaft mechanism of which the connecting rods of both the piston and the displacer join to the crank shaft by the same

journal bearing. This arrangement produces sinusoidal motion of both the piston and displacer with a phase angle, α, offset governed by the angle between the cylinder axes.

1.1.3 Advantages of Stirling engines

Stirling engines offer many advantages as an alternative method for energy conversion. Operation of a Stirling engine only requires an external heat source and sink to transfer the energy to and from in order to produce work. This allows the heat source to be anything that offers enough energy and temperature. Examples of potential heat sources can be conventional hydrocarbon fossil fuels such as gasoline, diesel, kerosene, non-conventional hydrocarbon fuels such as alcohol, wood, and other biomasses, as well as completely renewable resources such as concentrated solar rays. The irrelevance of combustion timing allows the combustion process to be modified for more complete combustion, increasing efficiency and reducing the output of harmful greenhouse gasses. Even

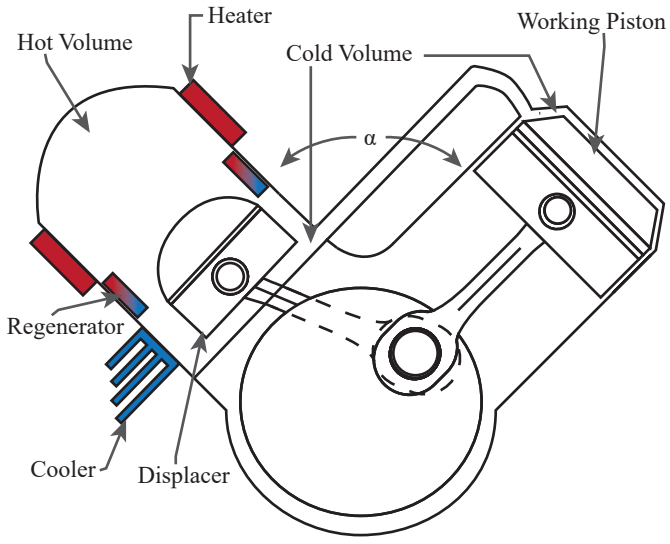

Figure 4. Schematic of an gamma-type Stirling engine.

if an application requires conventional fossil fuels to be used, the Stirling engine has the capability of using them in a more environmentally considerate manner.

Given that the Stirling combustion or heat addition process is externally applied, the noise commonly associated with internal combustion is non-existent. Therefore, Stirling engine operation is quiet in comparison to internal combustion engines. Experimental results have determined that the noise level of a 100cc Philips Stirling engine was 58.9dB which is comparable to a conversation in a quiet living room or office [4]. This characteristic allows the operation of the Stirling engine to be in close proximity, perhaps even indoors, to the end user. Furthermore, in minimizing the distance between the generator and the user, the losses from electricity transport are lessened.

The closed-loop operation of Stirling engines provide an opportunity to use a working fluid other than air. The term working fluid refers to the gasses that reside within the engine that are thermodynamically manipulated to transfer energy. The default working fluid for any open-loop configuration is air, as the respiration with the atmosphere leaves the operation with no other option. The Stirling engine is able to operate on different working fluids, namely air (or pure nitrogen), helium, and hydrogen. Both helium and hydrogen have potential to offer a more power-dense option as the thermal conductivity is higher than air, increasing the effectiveness of the heat transfer within the engine. Additionally, hydrogen offers a viscosity value less than air and helium. This can reduce the pumping losses associated with fluid transport due to the viscous sheering effects within the engine components. Experimental results suggest that hydrogen and helium may allow for an increased net work over air, while efficiency values remain unchanged [4].

1.2 Stirling engine literature review

1.2.1 A brief history of Stirling engines

The first Stirling engine was invented in 1816 by Reverend Robert Stirling. In 1850, John Ericsson demonstrated a similar type of engine, of which operated on isobaric regeneration processes, that was able to power agricultural water pumps. By the World War I, Stirling engines were used as safe reliable sources of energy for applications from power sources for industrial units, to organ pumps and sewing machines [6]. Development of the external combustion engine was promoted in the mid 1900's as stainless steel became commercially available. Owing to it's corrosion-resistant property, the advent of stainless steel negated previous issues caused by excessive wear and component seizure due to oxidation, thereby allowing for long term operation. In the mid to late 1900's, Philips, General Motors, and Ford began showing interest in Stirling technology, an example is shown in Figure 5 with a prototype of a GM Stirling engine powered sedan. They produced engines far exceeding emissions standards of the day while operating on any grade of fuel without issues. The GPU-3 is an example of a 120cc generator unit able to provide portable energy at 4.5kW. The 4L23 is a four-cylinder automotive engine that produced 210kW and was able to propel a sedan while consuming 8L/100km of fuel [4]. These examples were all built with the piston(s) and a displacer constrained to a crankshaft, therefor producing sinusoidal motion. The widespread adoption of the Stirling engine has yet to materialize likely because efficiency values are not sufficient enough to disrupt current views on energy conversion.

1.2.2 Recent work in Stirling analysis

The Stirling cycle can convert heat into mechanical energy at efficiencies equivalent to Carnot efficiency [1]. Carnot is the maximum achievable efficiency for all heat engines, however in practice, Stirling engines have failed to achieve these high efficiencies and the deviation experimentally recorded is more than just the mechanical losses alone [4]. Many operational parameters have been explored by researchers to better understand the factors that contribute to losses in the practical Stirling engine. The following areas are often explored in hopes of improving Stirling technology; heater, cooler, and regenerator effectiveness [7], friction losses [8], dead volume [9], compression ratio [3], and the ability of the engine to follow the ideal thermodynamic Stirling cycle [10]. The following studies outline both analytical and numerical methods for quantifying and improving the net work produced from the Stirling engine.

Figure 5. 1979 GM AMC concept concord sedan with a Stirling power unit.

Analysis and modeling of sinusoidal Stirling engine performance

Following the invention of the Stirling engine, in 1871 G. Schmidt [11] was the first to develop an analysis that differed from the ideal Stirling cycle by introducing sinusoidal motion of parts coupled with a discrete isothermal analysis. His approach allowed for the analysis of various Stirling configurations such as the alpha, beta, and gamma-types shown in Figure 2, 3 and 4 respectively. Schmidt assumed that the heat addition was only during the expansion stroke which mathematically constrained the Stirling engine analysis to be equivalent in efficiency to Carnot. Schmidt later attempted to improve upon his analysis by incorporating an integration method to shorten computation time [4].

In the late 1800's Schottler and Zeuner [12] made assumptions about hot space and regenerator temperatures in an effort to increase Schmidt's accuracy. However, it was not until T. Finkelstein's heat transfer limited analysis [12], published in 1960, where a model was able to utilize power and pressure parameters to determine the effective heat transfer of the system. This allowed experimentalists to determine the effectiveness of their heat exchanger designs.

Walker and Kirkley in 1962 [13] [14] further expanded on Schmidt's work by comparing the total swept volume to the maximum cycle pressure to determine their version of a dimensionless power parameter. They used their analysis method to test several thousand values to determine the optimal proportions for the alpha, beta, and gamma Stirling engine configurations. They determined that a beta configuration designed to have displacer and piston spaces overlapping at times within the cycle, would allow it to

produce the most power and efficiency. The gamma Stirling engine shows the least in performance and efficiency characteristics.

Urieli and Berchowitz in 1984 [15] expanded Walker and Kirkley's calculations by adding the concept of a heat rejector and acceptor into the adiabatic or heat transfer limited model. This analysis enabled the modeling of heat transfer and pressure drop within heat exchangers to better predict the transient response of the Stirling engine.

Further analysis and accuracy extends past a closed form solution and requires numerical solvers capable of computing CFD and FEM models. In 2004 R. Dyson et al. [16] performed a comprehensive analysis on the accuracy and computational intensity of thermal-fluids solvers such as Fluent. This multi-dimensional solution enables a better understanding of the actual thermal-fluid flow in a Stirling engine.

The described studies thus far have driven the progression of analytical and numerical approaches, enabling a better understanding of the Stirling engine with regards to net work, heat transfer, and fluid flow within the engine. Although authors included sinusoidal motion of parts into their analysis, little focus was put towards Stirling engine efficiency and all conclusions on the matter ensue efficiency values equal to that of the Carnot cycle.

Improvements of the Stirling engine

An early venture into Stirling engine improvements was led by Theodor Finkelstein in 1960 [17], his first approach was to focus on varying both phase angle, α, and the volume ratio between the hot and cold spaces. He employed the isothermal model with sinusoidal motion of parts to eliminate dependencies on heat exchanger performance. He

described that the phase angle changes the compression and expansion periods, altering the thermodynamic step duration. His results show that selecting the correct parameters may double the net work of an engine in comparison to the standard arrangement. He concludes that this increase in engine throughput is due to an increase in compression ratio. However, his assumptions produce efficiency values equal to that of the ideal cycle.

To further attempt to generalize the Stirling analysis and produce meaningful characteristic parameters, Finkelstein continued his optimization criteria. In 1996, he introduced the concept of 'Tidal' and 'Ancillary' domains [18]. He defined dimensionless quantities for specific performance and compression ratio, which he described as; the amount of energy produced per unit mass within a pressurized Stirling engine and the compression characteristics of the Stirling engine that best resembles the compression ratio of an internal combustion engine. His conclusions are that the isothermal analysis precisely predicts a phase angle offset of $\pi/4$.

L. Erbay and H. Yavuz in 1997 [19] develop a set of equations for the Stirling cycle under maximum power conditions. This approach enhanced the previous models by treating the thermodynamic steps between the state points as polytropic. The authors use this approach to determine the optimal regenerator characteristics. They also concluded that an engine should be designed around maximum power density, rather than maximum power, as there is potential for higher efficiency.

F. Wu et al. in 1998 [7] took the adiabatic model with sinusoidal motion of parts and developed it to determine the optimum performance of a Stirling engine with finite heat exchanging time in both the regenerator and the heat exchangers. This approach showed that regeneration and heat transfer rates must be balanced to operate at a maximal

level. M. Costea et al. in 1999 [20] employed a similar model, however their focus was on solar-Stirling engines to show the irreversibilities in a renewable application.

In 2006 B. Kongtragool and S. Wongwises [9] developed the isothermal model with sinusoidal motion of parts to include imperfect regeneration and dead volumes within the hot space, cold space and regenerator. The regenerator temperature was assumed as the arithmetic mean of the sink and source temperature. They describe the scenario where regeneration is considered perfect, and conclude that dead volume affects net work only. In addition they describe that regenerator effectiveness affects both heat input and efficiency. Lastly, they conclude that if regeneration is considered perfect, the Stirling engine efficiency is equivalent to the ideal cycle.

In 2010 F. Formosa and G. Despesse [21] expanded on the development of B. Kongtragool and S. Wongwises's isothermal and sinusoidal study by including a dynamic response of a Stirling engine by defining kinematic and dynamic features. The aim was to take practical features such as dead volume, heat irreversibilities and non-ideal regeneration and pair it with general dynamic motion of the engine piston and displacer to understand the transient response of the system.

In a similar manor to past studies, in 2012 C. Cheng et al. [22] completed a isothermal study with sinusoidal motion of parts to find optimal geometric parameters including swept volume ratio and the phase angle, α, for the alpha, beta, and gamma-type arrangements. They focus on two practical variables; dead volume ratios, and temperature ratio. Their results were presented in multiple dimensions to show the local maximums in a multi-space domain. This approach determined that the beta arrangement prevails in all categories of scrutiny. In contrast to previous approaches they conclude that the alpha-

type arrangement was shown to have poor results in low temperature ratios, while the gamma was shown to be the most effective in low temperature ratios. They do not show how these values may affect thermal efficiency.

In 2013 H. Ahmadi et al. [23] was among some of the earliest authors to utilize machine learning algorithms to solve a multi-objective optimization methods and improve on the state-of-the-art optimization. They discuss various algorithms and employ a Non-Dominated Sorted Genetic Algorithm (NSGA) and use it to solve three different decision criteria; TOPSIS, LINMAP, and Bellman-Zedeh. Decision variables included RPM, pressure, entropy, source temperature, sink temperature, number of regenerators, lengths and diameter of the heat exchangers. Output variables included regenerator diameter, net work, efficiency, and pressure drop. All three decision criteria returned results that were similar, and correlated well with experimental data, producing single digit errors. Additionally this study revealed that if the decision weight of thermal efficiency was larger than the other objectives, a low temperature ratio can be considered.

In 2013 F. Formosa and L. Frechette [24] produced scaling laws in attempt to understand the size-ability of the technology, focusing on miniaturization. The authors develop characteristic dimensionless groups that they feel best represent the physics and geometric parameters of a Stirling engine; pressure, mass within hot/cold space, mass flow rate, temperature, time, and length. The authors utilized Schmidts equations coupled with gas dynamic equations to make dimensionless comparisons. The conclusions suggest that power density increases with miniaturization however leakage adversely affects small-scale engines far worse than standard sized Stirling engines.

The described studies in this section have developed general Stirling engine improve-

ments that may increase Stirling engine performance. The piston movement in these studies were also constrained to a crankshaft resulting in sinusoidal motion. No authors investigated sinusoidal motion as an influence on performance reductions, and little effort was applied to determining the affects of their improvements on engine efficiency.

Design specific analysis

The studies presented in the previous section of this thesis outlines the chronological development of improvement techniques that apply generally to all types of Stirling engines and layouts. These studies present useful tools to aid in understanding the core functions of the Stirling engine. Many more studies focusing on improvements have been done in parallel to the general studies but with an emphasis on specific geometric features and application specific Stirling engines.

In 1999 K. Mahkamov and D. Ingham [25] performed an analysis of the mechanical losses for a solar powered Stirling engine. This study analyzed a theoretical 1 kW gamma-type stirling engine that was divided into five main sections; the heater space, expansion space, regenerator, cooler space and compression space. A set of ordinary differential equations were used to quantify the thermodynamics, and coupled with a sinusoidal dynamic model to resolve the friction forces and the subsequent losses. They resolved an indicated and brake power of 3190 W and 1585 W respectively with an electrical converted power of 998 W, concluding a 50% net work reduction from mechanical losses alone. Of the total losses 63% were said to be from the piston rings. The authors suggest a total 26 - 27% overall increase can be achieved by utilizing a single piston ring sealing solution.

K. Mahkamov in 2006 [5] used his previously published approach coupled with CFD in attempt to further understand the performance of an existing biomass fired gamma-type Stirling engine. The manufactured engine was designed using an isothermal model and was underperforming. Mahkamov utilized his approach to resolve that dead volume was likely the reason. The obligatory heat exchanger design forced Mahkamov to improve the engine with an alpha-type redesign, which later produced the targeted manufacturer net work values.

In 2007 C. Cinar [26] presented a theoretical alpha-type Stirling engine model for both kinematic and thermodynamic analysis utilizing nodal analysis in FORTRAN to resolve the effects of phase angle, α, on net work. The 170 cc alpha-type Stirline engine operated on a crankshaft and was simulated to have 200, 300, and 400 W/m^2K convective heat transfer coefficients in the heat exchangers, while examining phase angles of 80, 90 and 100. He found that the 80 degree phase angle produced a higher compression ratio, however it suffers during the expansion and compression strokes due to shortened duration's. The 100 degree phase angle was able to thermodynamically benefit during compression however suffered from a lack of expansion ratio. He concluded that 90 degrees was the most advantageous compromise. He did not mention how these changes may have affected thermal efficiency, though they altered the thermodynamic steps.

C. Cheng and Y. Yu in 2010 [27] developed a numerical model for a beta-type Stirling engine with an annular gap type regenerator and a rhyombic drive mechanism. This mechanism produces in-line sinusoidal movement for both the piston and displacer, allowing for a compact design. The authors developed the fluid mechanics equations for flow between the displacer and the cylinder under oscillatory conditions governed by si-

nusoidal motion. This enabled the analysis of the internal irreversibilities caused by the regenerative flow resulting from a viscous shear effects through the annular gap. They determined that their engine can operate between 13.1% and 16.5% efficiency at maximum performance and efficiency configurations by varying the gap from 0.0005 to 0.0003 m respectively at a 600 K hot temperature constraint. These values are far lower than Carnot efficiency and fluid flow losses alone, and further reasoning was not discussed.

In 2012 M. Campos et al. [28] presented a simplified two cylinder sinusoidal swash-plate driven Stirling engine for analyzing both the classical thermodynamics as well as heat transfer with variable heat transfer coefficients. The authors expanded on a previous publication by using the results from the first model to simulate the transient and steady state engine response. They identified two significant dimensionless parameters that affected results; the ratio between total expansion volume and total swept volume, and the ratio between the heat transfer area of the hot heat exchanger and the total heat exchange area. Optimal values for the dimensionless parameters were fount to be 0.5 and 0.4 respectively.

In 2014 J. Bert et al. [29] tested a 1 kW gamma-type Stirling engine with both air and helium as the working fluids. They studied the influence of the working pressure, engine speed and the hot side temperature on net work. Test results were used to validate a finite-time thermodynamic model, and a kinematic optimization criteria was put in place to find additional net work. Rudimentary optimized P-v diagrams are presented. The authors estimate that motion outside the conventional connecting rod and cranking mechanism, producing non-sinusoidal motion, may result in up to a 22% increase in power. Their analysis lacks depth, as they omitted efficiency from their calculations and

the motion was not plausible in a real engine design.

In 2016 S. Alfarawi et al. [30] developed a CFD model around a 500 W gamma-type Stirling engine with the regenerator and cooling spaces treated as porous domains. Given the relatively small characteristic size of the regenerator and cold heat exchangers, the authors attempted to increase the accuracy of both the viscous losses and the heat transfer by determining an equivalent porosity. This approach proved to return an error between 9% and 5% for the cooler and regenerator respectively. This method was then used to find an optimized phase angle, α, resulting in 105 degrees for this particular design, and the optimal displacer to power piston connecting pipe diameter.

In 2016 M. Briggs [10] published analysis and experiments on demonstrating potential benefits of optimizing piston and displacer motion in a free piston beta-type Stirling engine. Briggs utilized isothermal nodal analysis to determine that the sinusoidal cycle motion can be improved upon. His analysis predicts up to a 58% increase in power if both the piston and displacer motion operates on higher order harmonic motion, effectively mimicking dwell. His movement modification can be seen in Figure 6. By utilizing a beta-type test engine and developing a control system that is able to keep the electromagnetic coupling while modifying the component movement to mimic dwell, Briggs is able to determine fluctuations in power output. Experiments show a 14% increase in net work when the engine was forced to operate on either the second or third harmonics. His experiments also concluded that efficiency was negatively impacted, however the reasons were not discussed.

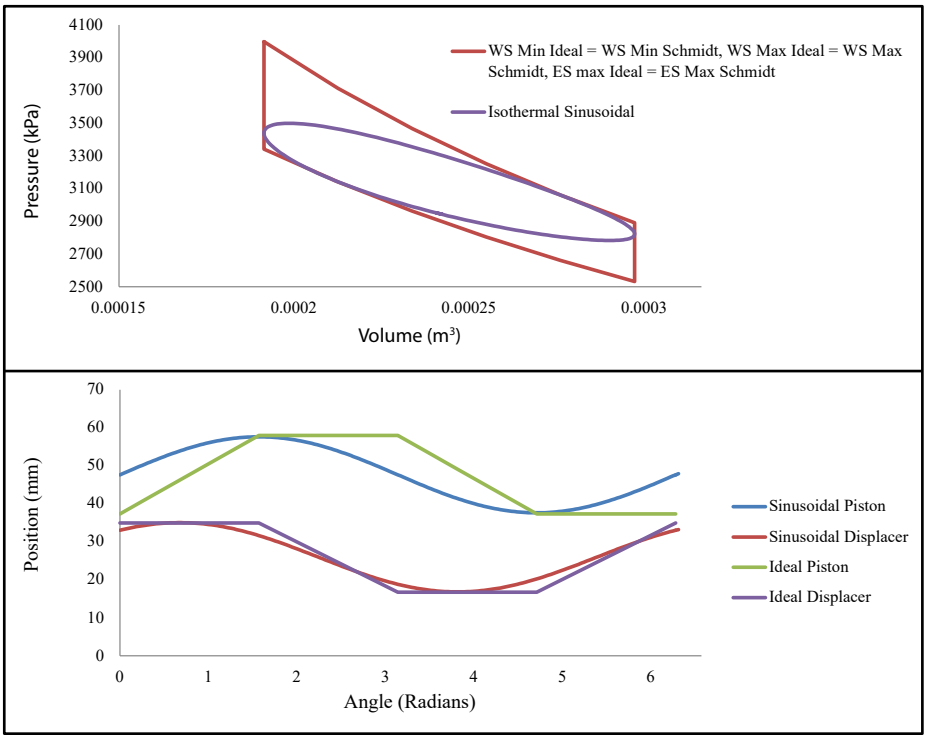

Figure 6. A *P-V* (top) and *Position-Angle* (bottom) for one of M. Briggs piston and displacer movement cases for increasing Stirling engine power [10].

1.3 Gaps in the literature

Many of the aforementioned studies developed methods to analyze and optimize Stirling engines, utilizing different approaches that apply both generally and specifically. These analyses cover a wide range of constraints and analyze discrete and global thermodynamic properties as well as heat transfer parameters to find increases in net work. Although net work is an important parameter, and often a commercially driven feature, efficiency is ultimately the long term determining factor to an economically viable solution and should be focused on. Many studies have included sinusoidal motion into their analysis, however they have omitted the investigation of efficiency reduction, and in addition several studies have alluded to the importance of designing engines around efficient operation.

The Stirling engine is a approximation of the Stirling cycle, in that designers take the ideal operations and represent the thermodynamic theory with a mechanical design. Often times the most familiar and robust mechanisms are simple to design and implement into a technology. However, in the standard Stirling configurations the sinusoidal movement of both piston(s) and displacers constrained to crankshafts, to transfer linear motion to rotational motion, may accompany non-ideal thermodynamic outcomes. Furthermore, experimental evidence reveals a substantial deviation of efficiency from the acclaimed ideal or Carnot cycle. To the best of my knowledge no study breaks down the operation of the sinusoidal Stirling cycle to address any thermodynamic inconsistencies, and how those deviations affect efficiency.

1.4 Thesis objectives

The objective of this thesis is to model and discretize the sinusoidal Stirling cycle with the isothermal assumption to enable the analysis of work, and heat inputs and outputs to determine the resulting efficiency values. This model can then be used to accomplish the following items:

- Uncover the deviations of the sinusoidal operation from the true Stirling cycle.
- Quantify the losses associated with a sinusoidal engine for the standard α, β, and γ configurations.
- Demonstrate the plausibility of having a Stirling engine design that can operate with non-sinusoidal behaviour.

Chapter 2

Thermodynamic modeling

In this chapter, the Stirling engines qualitatively described in the previous subsections will be quantitatively explored. All of the operational parameters are set to provide a realistic example of a Stirling engine that can be used in practical applications. The equations for the intensive and extensive thermodynamic properties are mathematically described and isothermal assumptions are employed. The energy analysis method is also mathematically described and then illustrated in later sections of this thesis.

2.1 Engine description

The initial thermodynamic model is built around the alpha-type Stirling engine configuration shown in Figure 2, which comprises of individual compression and expansion piston-cylinder devices that share a common cranking mechanism with the connecting rods joined at the same location. The phase angle which provides the piston motion offset, α, is the angle between the two cylinder banks and can be seen in Figure 2. This

arrangement results in continuous sinusoidal operation. In order to begin to quantify the system parameters, the isothermal assumption is employed, which considers the working fluid temperature in either the hot or cold space to be equal to the source and sink temperature.

The Stirling engine in this analysis was sized to provide power for a residential or small scale agricultural application and used as a reference to quantify results. The engine parameter values are listed in Table 1 outlining the engines cold and hot swept volumes, charge pressure, dead volumes, and temperature limitations that are set by the isothermal assumption. The total dead volume refers to the unswept volume, which is consequential to the maximum attainable compression ratio and often a indicator for power density [10]. It is necessary to include a small amount of dead volume as obligatory features such as piston clearances, regenerator volume, and heat exchanger volumes are always present in Stirling engine designs regardless of the piston(s) or displacer arrangement. The total mass of the working fluid was determined by treating it as an ideal gas at standard atmospheric conditions, and taken as if assembled at maximum engine volume while the phase angle, α is set to 90°. The analysis was also performed for various temperature ratios to demonstrate that the conclusions from this study apply generally and not specifically to the engine temperatures listed. Additional features such as journal pin offset, connecting rod length, and other specific engine features are omitted from the calculations as this would make the analysis specific to a particular engine geometry and detract from the general scope. The assumption that makes this possible is by assuming the the connecting rod length is much larger than the journal pin offset, resulting in pure sinusoidal movement of the piston(s) and displacer.

Table 1. Details of the engine used in the analysis.

Parameter	**Value**
Working Fluid	Air
Cold Swept Volume (cm^3)	100
Hot Swept Volume (cm^3)	100
Phase angle (°)	90
Charge Pressure (kPa)	101.325
Regenerator/ passage volume (cm^3)	2
Total dead volume (cm^3)	2
Hot Volume temperature (K)	773.15
Cold Volume temperature (K)	298.15

2.2 Discretization approach

In order to quantify the impact of sinusoidal motion constrained by a crankshaft, the divergence from the ideal cycle must be analyzed. The approach is to divide a full oscillation for both of the cycles into discrete crankshaft intervals, and analyze the volumetric changes and the associated thermodynamic intensive and extensive properties of the system. This provides a snapshot of the entire system at every interval so that the thermodynamic steps (mentioned in the introduction chapter) can be investigated. Initially the engine begins the rotation of the cycle with the hot piston at top dead center, corresponding to $\theta = 0°$ with the compression piston half way up the cylinder. The calculations are performed using incremental steps of 5° for the crank angle θ. This step size was validated by Martini [4] in his numerical analysis, to generate less than 0.5% error when compared to the isothermal analytical solver.

2.2.1 Calculating the system variables

The total system volume, V_{total}, is divided among the hot, regenerator, and cold volume, denoted as V_H, V_R and V_C respectively. They are expressed as a function of the crank angle position, θ, where 0° refers to the hot piston at top dead center, according to:

$$V_{total}(\theta) = V_H(\theta) + V_R + V_C(\theta). \tag{2.1}$$

The pistons follow sinusoidal motion, so the volume of each compartment varies with crank angle position according to:

$$V_H(\theta) = \frac{V_{H,max}}{2} * (1 - \cos\theta) + V_{DH}, \tag{2.2}$$

$$V_C(\theta) = \frac{V_{C,max}}{2} * (1 - \cos(\theta - \alpha)) + V_{DC}, \tag{2.3}$$

where α is the phase angle difference between the pistons, and V_{DH} and V_{DC} are the dead volumes associated with the hot and cold volume respectively.

The total mass of the system, m_{system}, is equivalent to the mass of the working fluid located in the hot volume, regenerator, and cold volume, denoted as m_H , m_R and m_C respectively:

$$m_{system} = m_H(\theta) + m_R(\theta) + m_C(\theta). \tag{2.4}$$

Specific volume for the system, v, can be computed as a function of the crank angle:

$$v(\theta) = \frac{V(\theta)}{m_{system}}. \tag{2.5}$$

By substituting ideal gas expressions for the mass associated with the individual engine compartments into Equation (2.4), engine pressure can be solved as a function of crank angle:

$$P(\theta) = \frac{m_{system} * R}{\left(\frac{V_H(\theta)}{T_H} + \frac{V_R}{T_R} + \frac{V_C(\theta)}{T_C}\right)}. \tag{2.6}$$

Pressure is considered to be uniform throughout all of the engine compartments at each point in the cycle. The constant, R, is the ideal gas constant.

The effective fluid regenerator temperature, T_R, is calculated as the log mean temperature as follows [4]:

$$T_R = \frac{T_H - T_C}{\ln \frac{T_H}{T_C}}. \tag{2.7}$$

The entropy change of the system is calculated utilizing the variable specific heat reference entropy, and can be written in terms of crank angle, θ, as follows [1]:

$$s(\theta) = s * (T_{global}(\theta - \Delta\theta)) + s^{\circ} * (T_{global}(\theta)) - s^{\circ} * (T_{global}(\theta - \Delta\theta)) - R * \ln\left(\frac{P(\theta)}{P(\theta - \Delta\theta)}\right), \tag{2.8}$$

where entropy associated with θ is the current crankshaft position and $\Delta\theta$ is the 5° crankshaft increment.

The global temperature is defined as the mean temperature across the whole system as follows:

$$T_{global}(\theta) = \frac{P(\theta) * V_{total}(\theta)}{m_{system} * R}. \tag{2.9}$$

2.2.2 Calculating the energy transfer

As mentioned in the introduction section, the ideal Stirling cycle requires isolation of the working fluid in the hot and cold cylinders during expansion and compression respectively. In engines that have sinusoidal operation, the working fluid is located in both the hot and cold cylinders during the expansion and compression strokes. In order to capture the thermodynamic behavior resulting from a sinusoidal engine, the work done on and by the system for each of the pistons needs to be tracked throughout the entire cycle.

The calculation for the incremental work done at each step of the discrete crank angle values for the hot and cold cylinders as follows:

$$W_H(\theta) = P * \left(V_H(\theta + \Delta\theta) - V_H(\theta)\right), \tag{2.10}$$

$$W_C(\theta) = P * \left(V_C(\theta + \Delta\theta) - V_C(\theta)\right). \tag{2.11}$$

The heat input is then calculated corresponding to the work values such that at each step where the work is a positive value in either cylinder, there is considered to be a heat input to the system:

$$Q_{in} = \sum W_H(\theta) > 0 + \sum W_C(\theta) > 0. \tag{2.12}$$

Similarly, for the heat output:

$$Q_{out} = \sum W_H(\theta) < 0 + \sum W_C(\theta) < 0. \tag{2.13}$$

The net work output resulting from a complete cycle can be calculated as follows:

$$W_{net} = Q_{in} - Q_{out}. \tag{2.14}$$

2.2.3 Mass calculation

The sinusoidal operation of the engine results in the working fluid located in both the hot and cold cylinders during the compression and expansion strokes, as described previously, but there is also potential for non-ideal mass transfer back and forth the between the cylinders during engine operation. To capture this behavior in this model, the mass occupying the compression, expansion, and regenerator volume at each of the discrete crank angle values are calculated as follows:

$$m_C(\theta) = \frac{P(\theta)V_C(\theta)}{RT_C}, \tag{2.15}$$

$$m_H(\theta) = \frac{P(\theta)V_H(\theta)}{RT_H}, \tag{2.16}$$

$$m_R(\theta) = \frac{P(\theta)V_R}{RT_R}. \tag{2.17}$$

2.2.4 Efficiency calculation

The thermal efficiency of the Stirling engine is calculated as follows [1]:

$$\eta_{th} = \frac{W_{net}}{Q_{in}}. \tag{2.18}$$

Chapter 3

Results and discussions

In this chapter the results from the thermodynamic modelling, outlined in Chapter 2, are presented and described. Energy illustrations in the form of P-v and T-s diagrams will show the thermodynamic behavior of the sinusoidal engine and reveal the deviations from the ideal cycle. The thermodynamic properties are compared concurrently to the engine cycle to understand why the deviations from the ideal cycle are occurring. Graphing the displacement of the piston(s) and displacer as well as the mass of the working fluid, throughout the cycle, will aid in the understanding of why the standard Stirling configurations cannot attain the ideal cycle efficiencies [31]. Lastly, an alternative arrangement is presented in the form of a cam-driven displacer beta-type variation, to deviate from sinusoidal motion. Analysis of this configuration will follow the same procedure to determine and quantify potential improvements in contrast to existing configurations.

3.1 P-v and T-s diagrams

Engine cycles can be visualized on P-v and T-s diagrams to illustrate their performance characteristics and visually represent the thermodynamic behaviour for both the work and heat transfer required to operate [1]. The P-v diagram illustrates the work within the cycle and allows for the quantification of work. The T-s diagram illustrates the heat transfer of the system. Both diagrams are useful to graphically understand the Stirling cycle as they allow analysis to be simultaneously seen from two sets of thermodynamic constraints. The cycle resulting from sinusoidal motion is plotted on the P-v and T-s diagrams in Figure 7, using equations (2.5), (2.6), (2.8) and (2.9). The ideal cycle is plotted using the same equations as the sinusoidal cycle but with fixed variables during the four ideal processes: isochoric heat addition (regeneration), isothermal expansion, isochoric heat rejection (regeneration), and isothermal compression. The ideal cycle was also fixed to the maximum and minimum volume values produced by equation (2.5) to mimic the piston sizing and make a meaningful comparison. The region shaded in gray corresponds to the work that could have been produced if the cycle was not limited by the sinusoidal motion of the crank shaft. Additionally the gray shaded reagion shows how the working fluid deviates from the ideal path and the specific reasons for this reduction are described by examining each process individually in the following sub-sections.

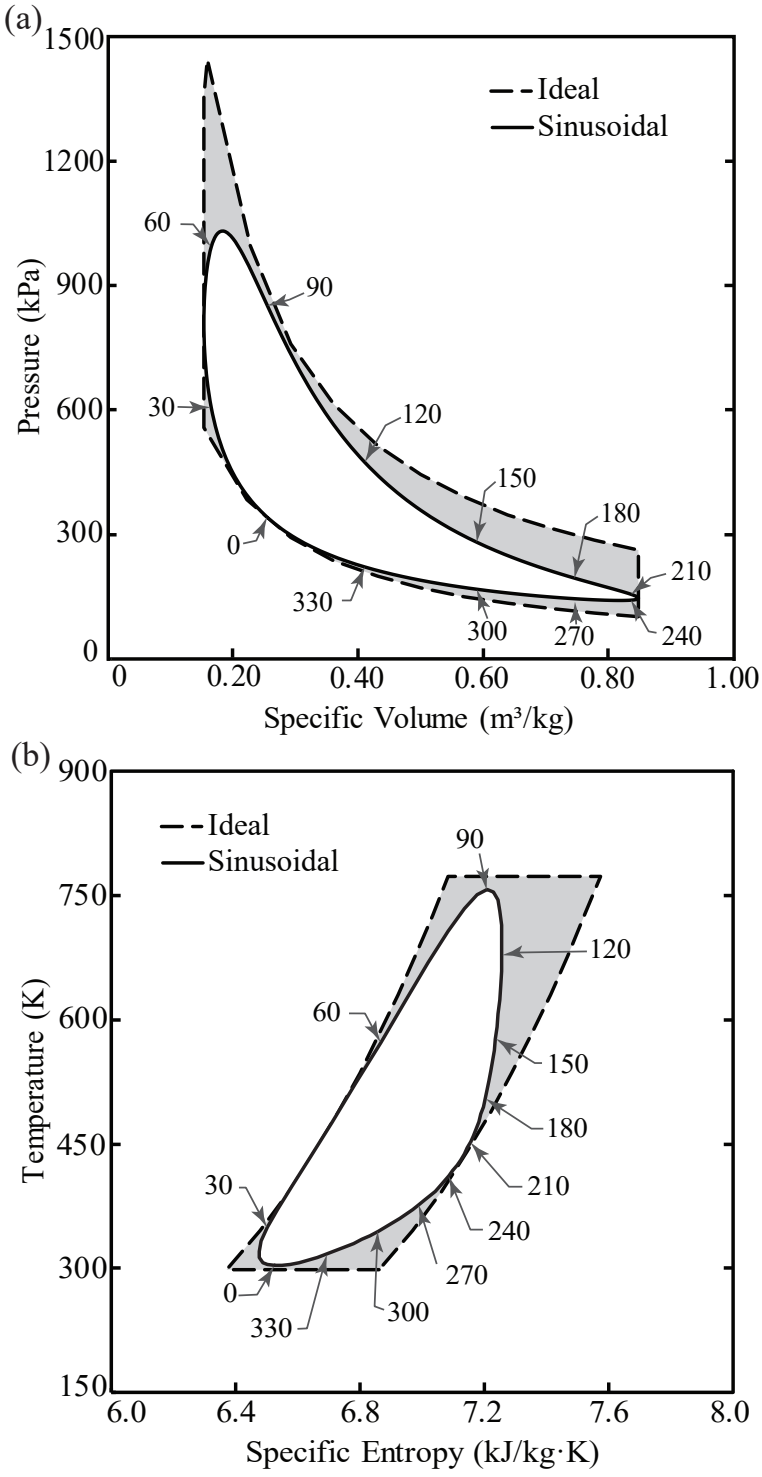

Figure 7. Sinusoidal and ideal cycle plots in (a) P-v and (b) T-s diagrams for the modeled alpha-type Stirling engine.

Isochoric regeneration (0°- 90°)

Crank angles from 0° to 90° correspond to the constant volume (isochoric) regeneration process, where in the ideal cycle, both pistons would move simultaneously, transferring the mass of the working fluid from the cold side of the engine to the hot side of the engine. In doing so, the working fluid would obtain the heat from the regenerator while producing zero net boundary work, and ideally results in a vertical line on the P-v diagram, as shown in Figure 7(a). However, with sinusoidal operation, the curve is rounded and only achieves constant volume for a small portion of the stroke, at 45°. For the sinusoidal cycle, the total volume of the system is plotted in Figure 8(a) alongside the individual volumes of the hot and cold pistons. The amount of mass of the working fluid located in each volume, and in the regenerator, is plotted in Figure 8(b). Figure 8(a) shows that the total volume is reducing from 0° to 45° and is increasing from 45° to 90°, due to the variation in the speed of the pistons, with constant volume only at 45°, corroborating the result in Figure 7. The increase in volume from 45° to 90° results in a decrease in the maximum pressure that can be attained, and as seen in Figure 7(a), the maximum pressure of the sinusoidal cycle is reduced from potentially 1445 kPa to 1032 kPa. This thermodynamic discrepancy reduces the potential net work of the system and can be witnessed by the gray shading in the upper left corner of both the P-v and T-s diagrams in Figure 7.

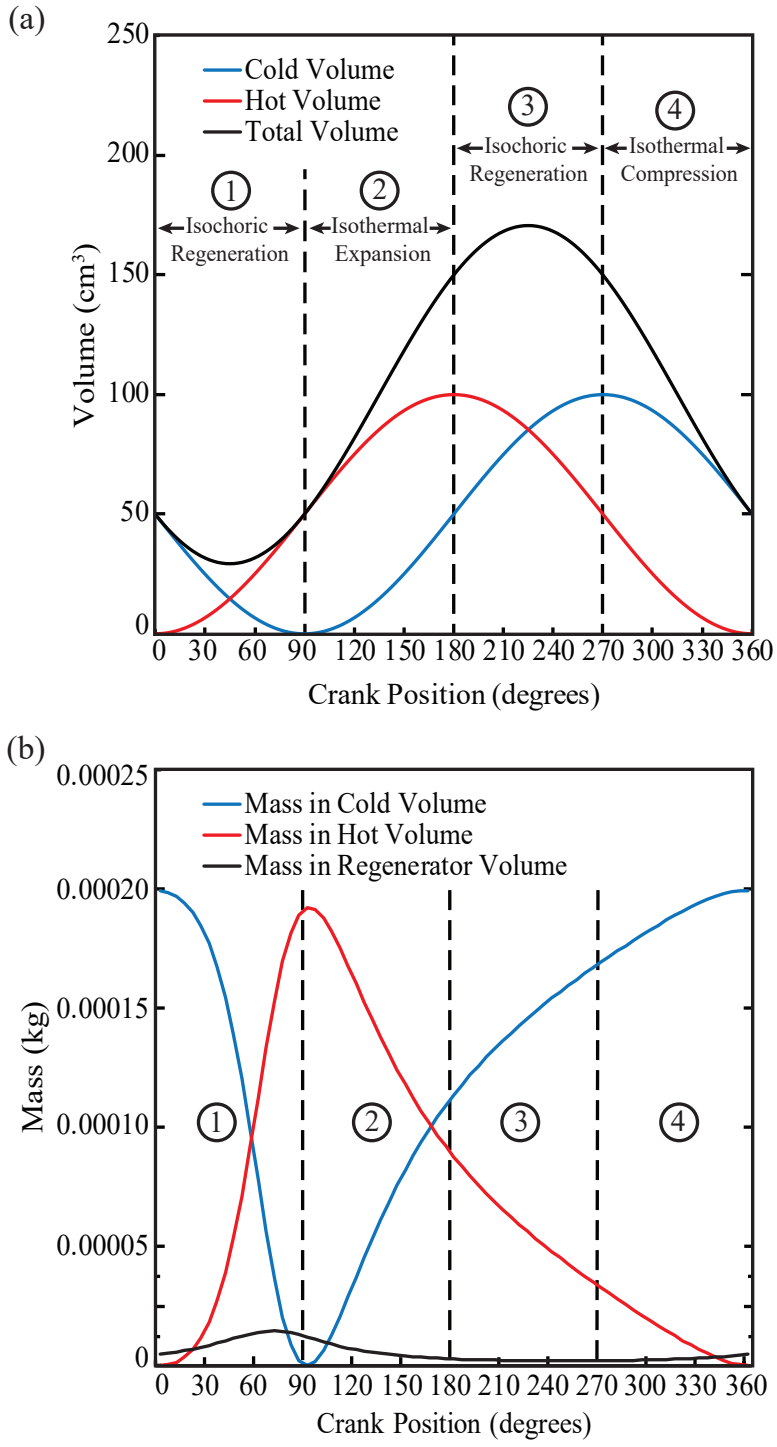

Figure 8. (a) Volume and (b) mass of the sinusoidal cycle as a function of crank angle (θ), for the alpha-type Stirling engine.

Isothermal expansion (90°- 180°)

Crank angles from 90° to 180° correspond to the work production process by isothermal expansion. In the ideal cycle, the working fluid would be isolated in the expanding hot volume while the hot piston travels along its stroke. However, in the sinusoidal cycle, this is only true for a small portion of the stroke, at 90°, where the working fluid is located almost entirely in the hot volume, as seen in Figure 8(b). Due to the continuous sinusoidal movement of both the hot and cold pistons, the working fluid is located partially in the cold volume during expansion, and just prior to 180° more than half of the mass is located in the cold volume, as shown in Figure 8(b). Expanding a mixture of both hot and cold fluid produces substantially less work than expanding only the hot fluid. This thermodynamic discrepancy results in the largest deviation between sinusoidal and ideal operation, and can be seen by the gray shaded region in the upper right corner of both the P-v and T-s diagrams in Figure 7.

Isochoric regeneration (180°- 270°)

Crank angles from 180° to 270° correspond to the constant volume regeneration process, where the hot working fluid is transferred across the regenerator and the heat is stored. In the ideal cycle this involves both pistons moving simultaneously while transferring the working fluid from the hot volume to the cold volume. In the sinusoidal cycle, the constant volume operation is achieved momentarily at 225°, with the volume increasing from 180° to 225° and decreasing from 225° to 270°, as seen in Figure 8(a). The volume variation prevents the sinusoidal cycle from following a straight downward line on the P-v diagram, as seen in Figure 7(a), and thus not following the ideal Stirling cycle.

Isothermal compression (270°- 360°)

Crank angles from 270° to 360° correspond to the work input by isothermal compression. In the ideal cycle, the working fluid would be isolated in the cold volume and the cold piston would travel from its maximum to its minimum volume. With sinusoidal operation, the compression stroke begins with some of the working fluid located in the hot volume, as seen in Figure 8(b), which increases the work input required for the cold piston to complete the compression stroke due to the higher average specific volume of the working fluid. This deviation can be seen from the gray shaded area in Figure 7 in the bottom right corner of both the P-v and T-s diagrams.

3.2 Work and heat transfer

The analysis of the work thus far has been primarily qualitative, and in this section, the work and heat transfer is examined quantitatively. The work is plotted in Figure 9 versus the crank angle, and summarized in Table 2, for the hot and cold pistons separately.

In the ideal Stirling cycle, work output occurs only in the hot volume, and work input occurs only in the cold volume. This can be accomplished by having the cold piston

Table 2. Summary of work during each process for the alpha-type Stirling engine.

Crank Angle Range (θ)	**Process**	**Work Summation Value (J)**	
		Cold Piston Work	**Hot Piston Work**
0°–90°	Isochoric regeneration	−32.6	43.0
90°–180°	Isothermal expansion	16.3	24.9
180°–270°	Isochoric regeneration	8.0	−7.4
270°–360°	Isothermal compression	−11.5	−9.1
	Total	−19.9	51.5
	Net Work	31.6	

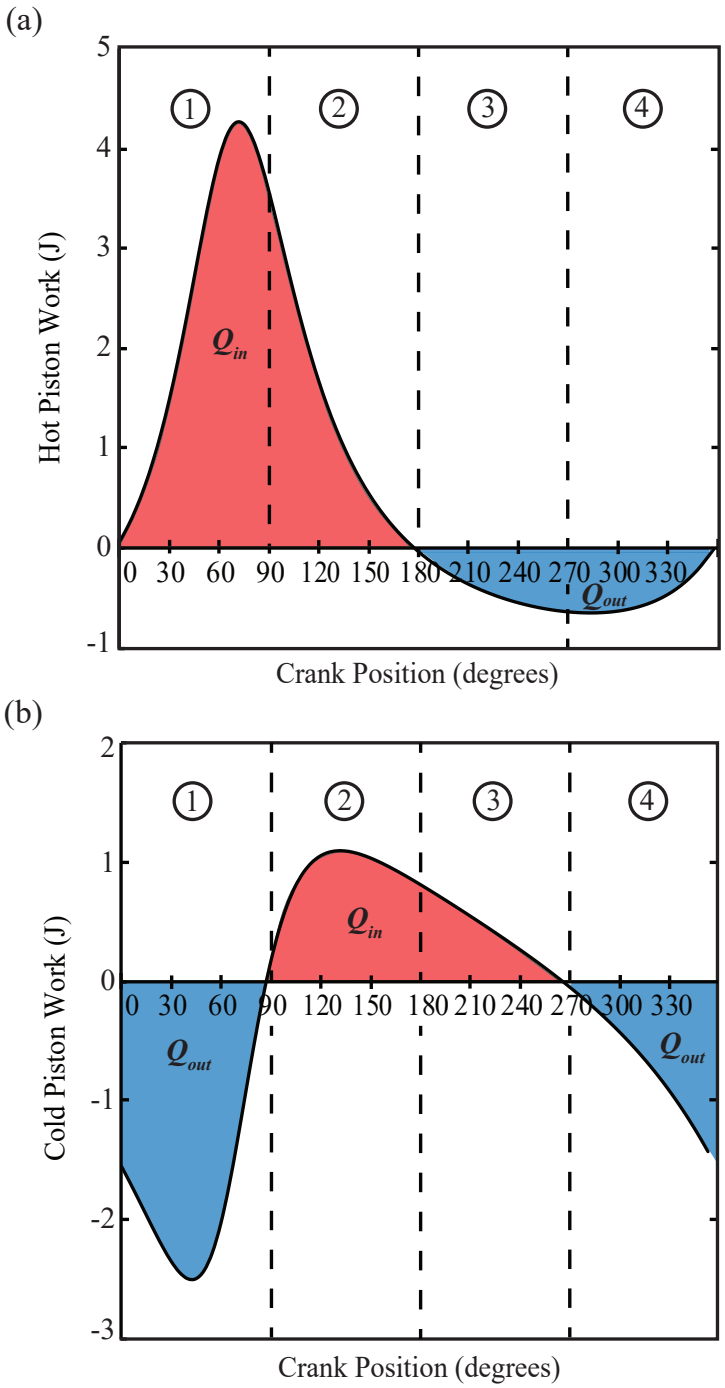

Figure 9. Work in the (a) hot cylinder and (b) cold cylinder versus crank angle (θ) for the alpha-type Stirling engine. The W_{out} corresponds to Q_{in} and is shown as red, and the W_{in} corresponds to Q_{out} and is shown as blue.

remain at rest during the expansion stroke, and the hot piston remain at rest during the compression stroke. During the isochoric regeneration processes, the ideal cycle would result in equal but opposite work profiles between the hot and cold pistons, cancelling the net effect. The sinusoidal cycle does not maintain constant volume during regeneration, as described above, and the pistons do not remain at rest during the expansion and compression strokes. To quantify the work that results from these deviations, Equations (2.10) and (2.11) are plotted in Figure 9.

The work is plotted in Figure 9 and the corresponding heat transfer is labelled as Q_{in} and Q_{out}, with Q_{in} shown as red and Q_{out} shown as blue. By analyzing the piston work shown in Figure 9 and Table 2, enables the quantification of the individual work and heat transfer from each piston during each process. Table 2 shows that the hot piston is responsible for the majority of the work output and corresponding heat addition, while the cold piston has more work input and corresponding heat rejection. However, due to the sinusoidal motion, the alpha-Stirling engine is only able to produce 31.6 J of work per revolution, which is only 65.9% of its theoretical limit, and thus the gray shaded region in Figure 7 corresponds to a 34.1% reduction in potential work output, for the values listed in Table 1.

3.3 Deviation from Carnot efficiency

The piston motion and corresponding working fluid location deviations described in the previous sections and graphically represented in Figure 7 not only affects the net work of the sinusoidal cycle negatively it also consequently impacts efficiency. During the thermo-

dynamic steps it is evident that the working fluid often partially resides in an unfavorable engine location therefore changing the properties of the fluid, namely the specific volume which is proportional to the work required to thermodynamically manipulate any fluid [1].

As shown in Figure 9, and described in Equations (2.12) and (2.13), the work output (expansion) corresponds to a required heat input and the work input (compression) corresponds to a required heat output, regardless of the cylinder of which this is occurring. Accordingly, using Equations (2.12)-(2.14), and (2.18), the thermal efficiency can be calculated. In the ideal cycle, this results in a thermal efficiency matching the Carnot efficiency ($\eta_{Carnot} = 1 - T_L/T_H$), which is 61.5% for the values listed in Table 1. For the sinusoidal cycle, the resulting thermal efficiency is 34.4%, which corresponds to a reduction of 27.1% from the maximum attainable efficiency.

Since the efficiency is strongly influenced by the temperature ratio, the efficiency is calculated for various temperature ratios to illustrate the deviation resulting from the sinusoidal cycle across a broad range of temperature ratios, as shown in Figure 10. Typically, a Stirling engine operates with a temperature ratio between 2 and 4, due to the material limitations, available heat sinks and fuel sources. Within these temperature bounds, the effects of sinusoidal operation on alpha-Stirling engines is reasonably constant as the resultant reduction in thermal efficiencies ranges from 23.6% to 29.5% respectively, as seen in Figure 10. This represents a substantial reduction in efficiency versus the theoretical efficiency and helps to explain why practical engines with sinusoidal motion have low efficiencies in comparison to the ideal efficiency. Operation with sinusoidal motion inherently limits the maximum attainable efficiency, and thus practical Stirling

engines operating with sinusoidal motion should be compared against this maximum efficiency as opposed to the Carnot efficiency.

3.4 Phase angle dependency for a sinusoidal alpha-type Stirling engine

Alpha-type Stirling engines operating on a sinusoidal cycle can use a variety of phase angles, α, which alters the expansion and compression characteristics and affects the maximum net work and attainable thermal efficiency for the system [26]. Based on the analysis, the net work and thermal efficiency is plotted against the phase angle in Figure 11, and illustrate how the phase angle influences the values. As seen in Figure 11, the phase angle that produces the maximum net work is 40°, which confirms the findings

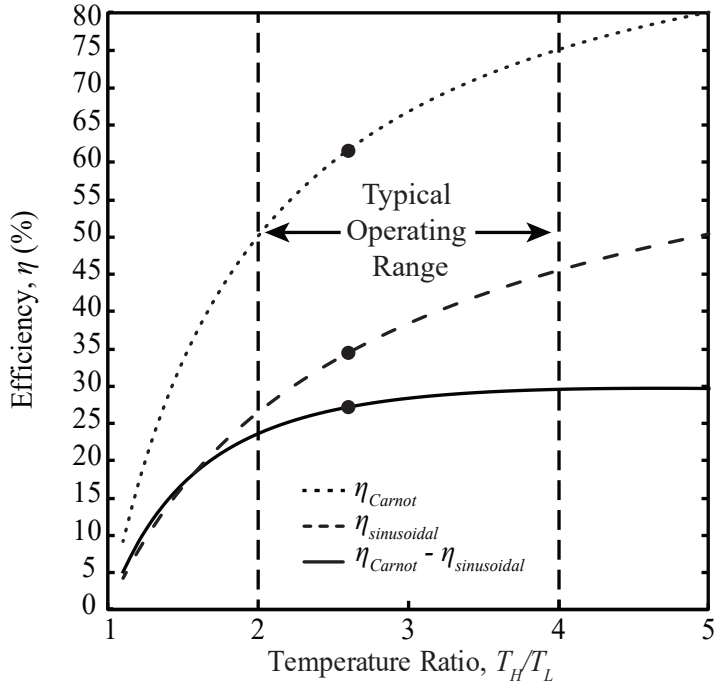

Figure 10. Efficiencies for Carnot, the sinusoidal cycle, and the deviation between them for an alpha-type Stirling engine at various temperature ratios. The point indicates the values corresponding to the engine details provided in Table 1.

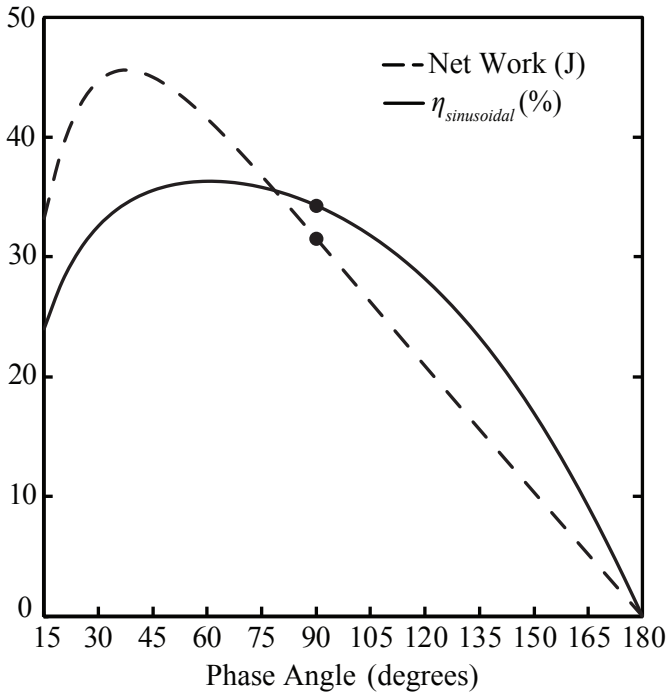

Figure 11. Net work and efficiency as a function of phase angle for an alpha-type Stirling engine. The points indicate the values corresponding to the engine details provided in Table 1, with a phase angle of 90°.

from past studies [26], producing 45.6 J per cycle, based on the values listed in Table 1. The analysis reveals that a phase angle of 60° corresponds to the largest attainable thermal efficiency, with a value of 36.4%. This is a small improvement over a phase angle of 90°, but ultimately still represents a substantial reduction versus the theoretical (Carnot) efficiency.

3.5 Effects of sinusoidal operation on beta-type and gamma-type Stirling engines

In order to numerically quantify the results thus far the previous sections were developed specifically for an alpha-type Stirling engine, as shown in Figure 2. However, the effects of sinusoidal operation are not limited only to the alpha configuration. The beta and

gamma-type Stirling engines are also common configurations [3]. Both the beta and gamma differ from the alpha configuration by their volumetric constraints, illustrated in Figure 3 and 4 as well as that the a single piston is responsible for both work input and output. While the hot volume remains identical to the alpha, the cold volume is not only constrained to sinusoidal movement with a phase angle shift, but also includes the relative location of the hot displacer or piston. This is reflected by a change in Equations (2.2) and (2.3) as follows:

$$V_H(\theta) = \frac{V_{H,max}}{2}(1 - \cos\theta) + V_{DH}, \tag{3.1}$$

$$V_C(\theta) = \frac{V_{H,max}}{2}(1 + \cos\theta) + \frac{V_{C,max}}{2}(1 - \cos(\theta - \alpha)) + V_{DC}. \tag{3.2}$$

Equations (3.1) and (3.2) describe both of the beta and gamma cycles, so the following analysis applies to both types. All of the other intensive and extensive thermodynamic properties and the associated equations remain the same as the alpha Stirling approach. The ideal beta and gamma Stirling cycles and the sinusoidal cycles are shown on the P-v and T-s diagrams in Figure 12.

The gray shaded regions show the areas of thermodynamic deviation due to sinusoidal operation that generate a reduction from the maximum potential net work and thermal efficiency. This is a result of the continuous sinusoidal movement of the hot and cold pistons and the inability to follow the ideal cycle, similar to the alpha-type Stirling engine, as detailed in the previous sections.

By applying Equations (2.12)-(2.14), and (2.18), and adapting them to apply to the

volumetric variations of the beta/gamma configuration with a power piston and displacer setup according to Equations (3.1) and (3.2), and using the values listed in Table 1, the

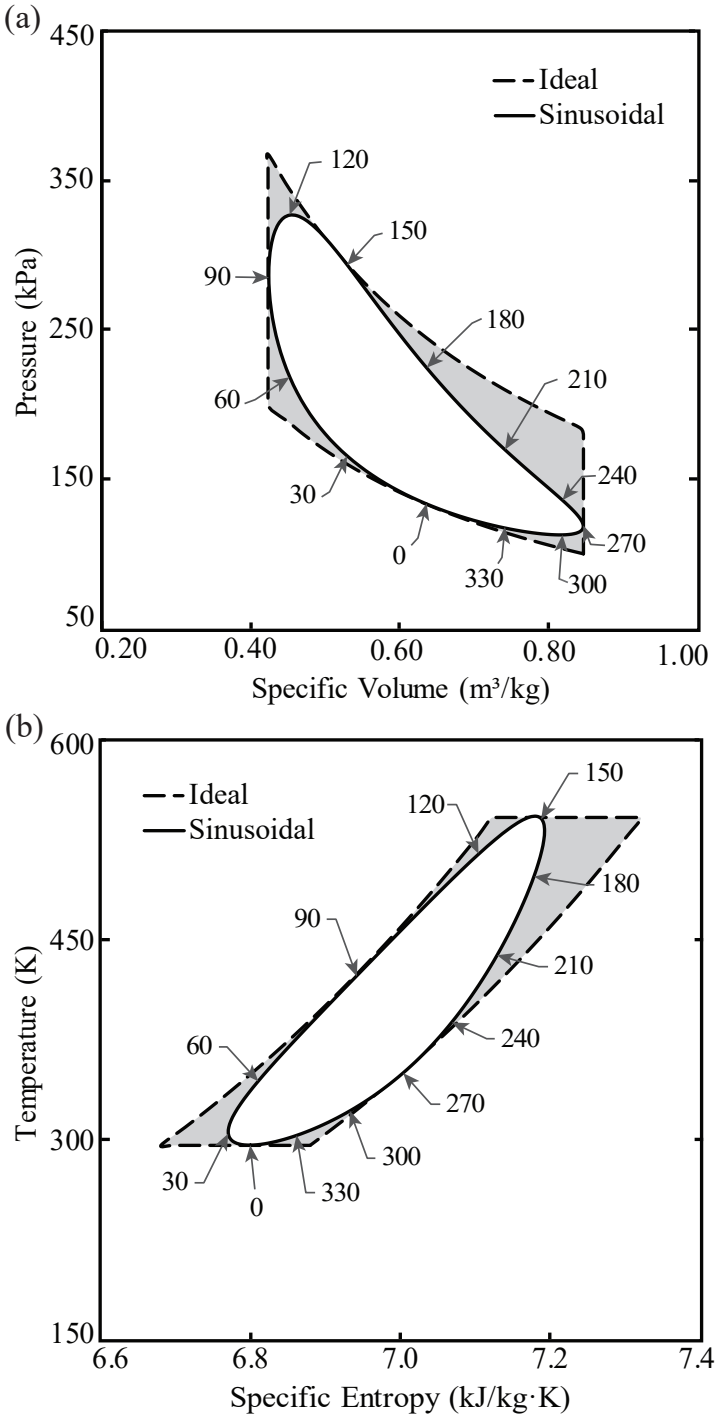

Figure 12. Sinusoidal and ideal cycle plots in (a) P-v and (b) T-s diagrams for the modeled beta and gamma-type Stirling engines.

thermal efficiency was found to be 35.8%, which is a reduction of 25.7% from the Carnot efficiency. Similar to the alpha-type engine, the efficiency depends on the temperature ratios, so the resulting efficiency is plotted for a range of temperature ratios in Figure 13. Within the typical operating range described above, the effects of sinusoidal operation on beta and gamma Stirling engines results in a reduction in thermal efficiencies ranging from 21.4% to 30.4% respectively, as seen in Figure 13. The findings demonstrate that sinusoidal operation impacts all Stirling configurations in a similarly adverse manner.

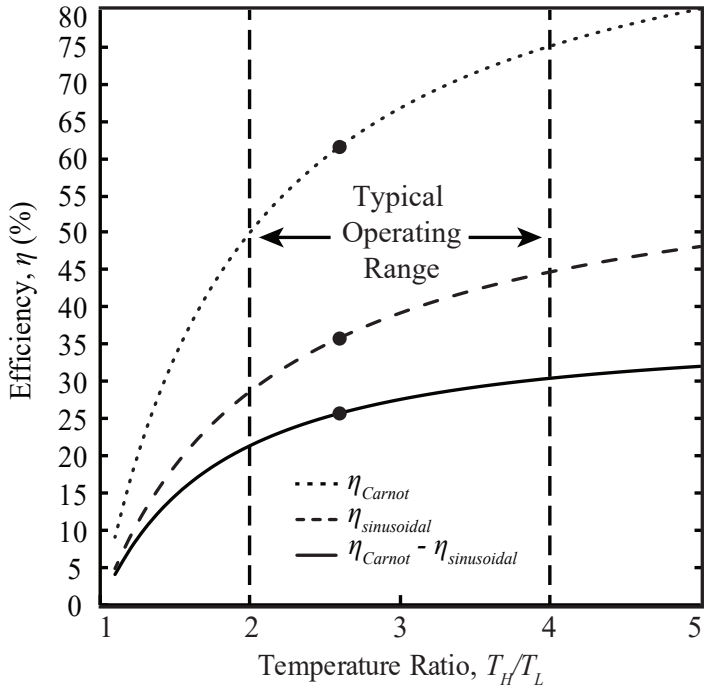

Figure 13. Efficiencies for Carnot, the sinusoidal cycle, and the deviation between them for both beta and gamma-type Stirling engines at various temperature ratios. The point indicates the values corresponding to the engine details provided in Table 1.

3.6 Non-sinusoidal Stirling cycle involving a cam

The analyses performed in the previous sections outline the thermodynamic shortcomings of the standard Stirling engine constrained to a sinusoidal movement. Based on Figures 10 and 13 the main parameter that can influence the efficiency of a Stirling engine is the temperature ratio, however even with a heat source and sink capable of wide modulation a trend of diminishing returns is notable. These reductions in both net work as well as efficiency are deterrents from the technology. Mechanical movement that differs from sinusoidal motion may offer the Stirling engine a more competitive advantage for both net work and thermal efficiency. Between any two temperature limits Carnot efficiency is the maximum attainable efficiency, and the ideal Stirling cycle is able to achieve the same values. Therefore, by producing a variation of the Stirling engine that better mimics the ideal movement, and can be mechanically possible, may allow for elevated efficiency. A simple yet plausible way to mechanically constrain Stirling engine components while deviating from sinusoidal motion is to utilize a cam driven mechanism, an example is shown in Figure 14.

Figure 14 shows a modified version of the beta-type configuration, with the displacer connected to a cam rather than a crank shaft while the piston remains constrained to sinusoidal motion. Cams offer a mechanical method for replacing linkages while allowing for irregular motion, with the advantage of tighter movement specifications [32]. In principal virtually any motion can be designed into a cam so long as the desired output is either linear or rotational, as cams produce a single degree of motion. The advantage of select engine components being constrained to a cam is that dwell can be integrated

into the component movement enabling the thermodynamic steps to happen in isolation. This may allow for more effective thermodynamic response as the volumetric variations may be able to better replicate the ideal Stirling movements. Because the Stirling engines components only experience linear motion a cam has the capability of offering an advantageous thermodynamic effect if implemented correctly. The drawback of implementing a cam in place of a crankshaft is the loss of ability to transfer torque effectively. To generate sufficient torque the mechanical system must be able to apply force at a tangent to a crank arm described by the equation; $\vec{\tau} = \vec{r} \times \vec{F}$, where $\vec{\tau}$ is the torque vector, $\vec{r}$ is the radial offset cranking length vector, and $\vec{F}$ is the applied force vector.

Stirling engines that utilize a displacer are good candidates for this mechanical modification. Knowing that the displacer is completely enclosed within the Stirling engine, it is subject to a zero pressure gradient resulting any motion and the subsequent the work equation $W = P(\theta)dV(\theta)$ to be zero [5]. Thus, if the displacer was constrained

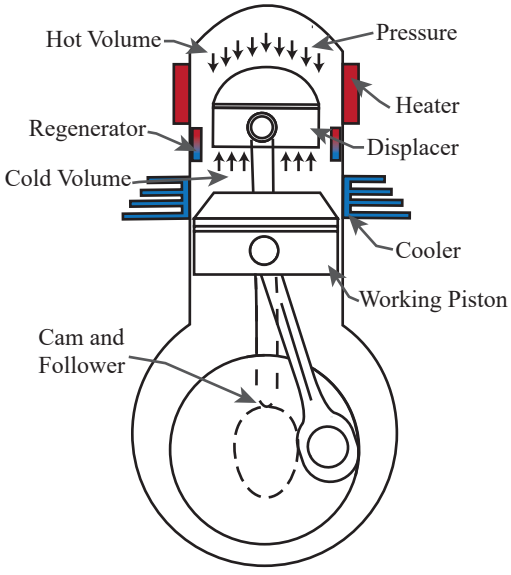

Figure 14. Schematic of a beta-type Stirling engine with an arbitrary cam driven displacer.

by a cam, little work would have to be put into the system to manipulate the displacer position. Additionally the displacer is capable of producing its own artificial spring to retain pressure onto the cam due to its inherent geometry. Although pressure is uniform, the surface area of the displacer differs slightly from top to bottom due to it's linkage. This linkage occupies some of the surface area, and when pressurized the displacer has a tendency to be forced down towards the crank shaft due to this difference in surface area as shown by the pressure arrows in Figure 14. In contrast, the piston must be able to effectively transfer torque and could not be driven by a device that only offers one degree of freedom. This makes both the beta and gamma-type Stirling engine configurations good candidates for the preliminary exploration of a non-sinusoidal Stirling engine.

Stirling engines operate at high rotational speeds, therefore to minimize vibrations and jerk within the system cams that are used in engines must be constrained to cyclodial motion according to the following equation, in dimensionless form:

$$\frac{y(\theta)}{L} = \frac{\theta}{\beta} - \frac{1}{2\pi} sin \frac{2\pi}{\beta}. \tag{3.3}$$

The incremental and discretized displacement $y(\theta)$ is location of the leading edge of the cam and therefore the follower of the displacer. The total rise of the movement is L, which for an engine is equivalent to the stroke of the displacer. The period of the rise or fall of the movement is β. Lastly, θ is the incremental and discretized angular displacement of the crankshaft and therefore the cam, as they rotate together, and is taken as 5° as previously discussed. Equation (3.3) returns a value from 0 to 1 in the nondimensional form, where 1 has the the displacer sitting at the bottom of its displace-

ment and therefore opens the hot volume to its maximum and 0 has the displacer sitting at the top of its displacement and therefore closes the hot volume to its minimum. The design of the cam will then be inverted to match the profile in the equal but opposite fashion. The hot volume defined in equation (3.1) can be rewritten to follow a cam rather than a crankshaft as follows:

$$V_{H,cam}(\theta) = V_{H,max}\Big(\frac{\theta}{\beta} - \frac{1}{2\pi}sin\frac{2\pi}{\beta}\Big) + V_{DH}. \tag{3.4}$$

The cold volume of equation (3.2) will still need to account for the relative location of the displacer and therefore can be expressed as:

$$V_C(\theta) = \frac{V_{C,max}}{2}(1 - \cos(\theta - \alpha)) + V_{H,max}\Big(1 - \frac{\theta}{\beta} + \frac{1}{2\pi}sin\frac{2\pi}{\beta}\Big) + V_{DC}. \tag{3.5}$$

Simulations reveal that the duration for β was found to be 74.1° for the rise and 78.5° for the return of the displacer cam. While the dwell associated with the rise is 105.9° and the dwell associated with the return is 101.5°. This produced the most efficient operation while keeping the cam within a size and pressure angle within a reasonable amount for the size of this engine. Theoretically, the rise and fall could happen within a shorter duration, producing a better efficiency and net work values, however this increases the angle of which the follower needs to abide by according to the following equation:

$$\phi = \arctan\Big(\frac{\Delta y}{r\Delta\theta}\Big). \tag{3.6}$$

Where r is the average radius of the cam for the interval. To perform a meaningful comparison, all of the other intensive and extensive thermodynamic properties and the associated equations remain the same as the previous approaches. The ideal and the partial cam-driven Stirling cycles are shown on the P-v and T-s diagrams in Figure 15.

The gray shaded regions show the areas of thermodynamic deviation between the cam-driven displacer with a sinusoidal piston operation that generates a reduction from the maximum potential net work and thermal efficiency. In comparison between the fully sinusoidal beta and gamma-type engine versus the half cam driven variation it is notable that the isothermal compression, and isochoric heat addition follow the ideal line almost exactly. This generates a larger pressure surge after regeneration and increases the maximum pressure from 328kPa to 456kPa. The largest deviation from the ideal cycle is shown in the top right corner of the P-v and T-s diagrams of Figure 15. This deviation occurs because of the relative location between the displacer and the piston during expansion and illustrated in Figure 16.

Figure 16 helps to explain the thermodynamic deviation from the ideal Stirling cycle shown in the the upper right corner of the P-v and T-s diagrams of Figure 15. After the isochoric heat addition, the expansion begins with all the volume open in the hot space and therefore all of the mass of the working fluid is on the hot side. As the expansion begins the relative location between the piston and displacer opens, and because the displacer is already in the lowest location there is an immediate loss of fluid mass to the cold side during expansion. This is shown in the 2nd thermodynamic step and causes a large pressure loss during expansion, limiting the cam driven displacer configuration. This issue exists both in this design as well as the full sinusoidal design. Despite this loss

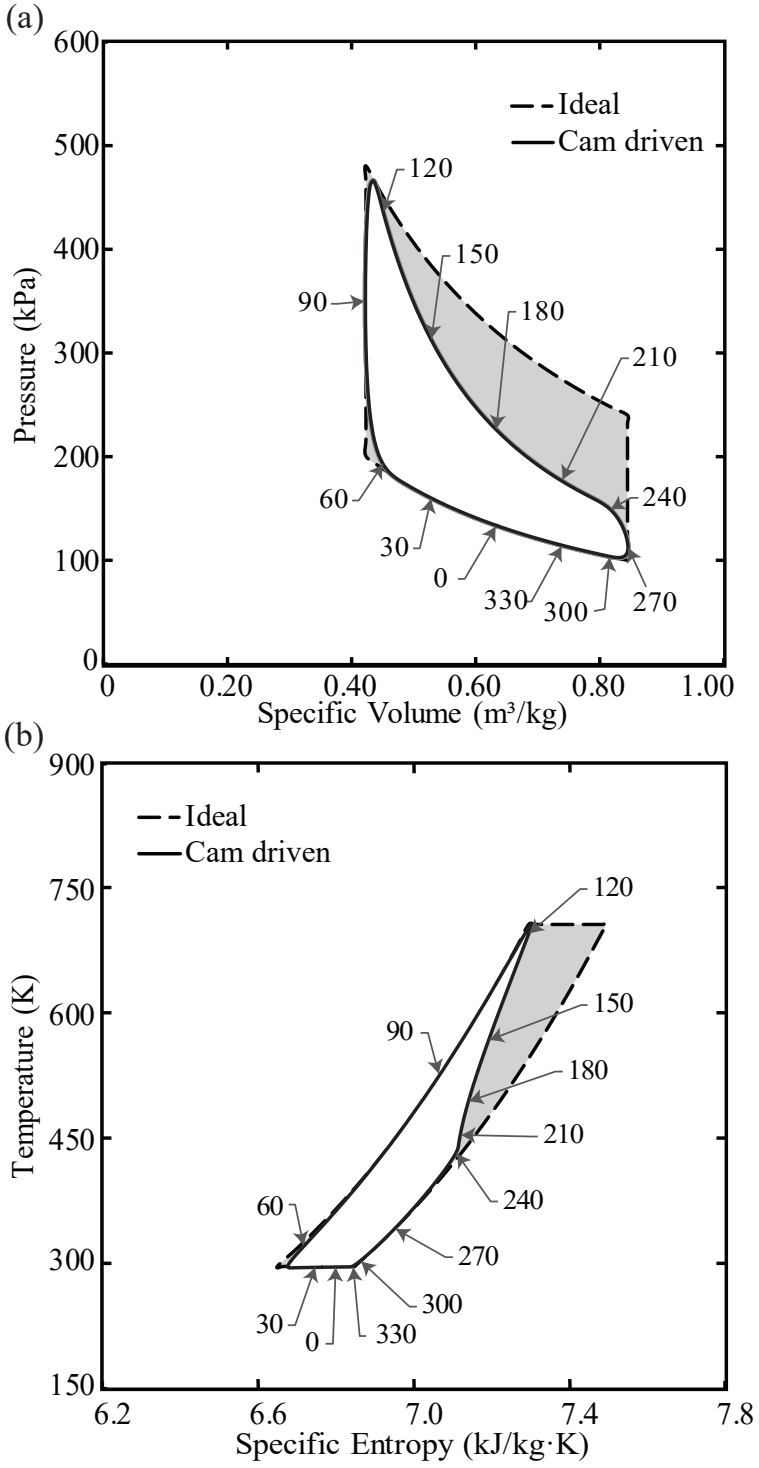

Figure 15. Cam driven and ideal cycle plots in (a) P-v and (b) T-s diagrams for the modeled beta and gamma-type Stirling engines.

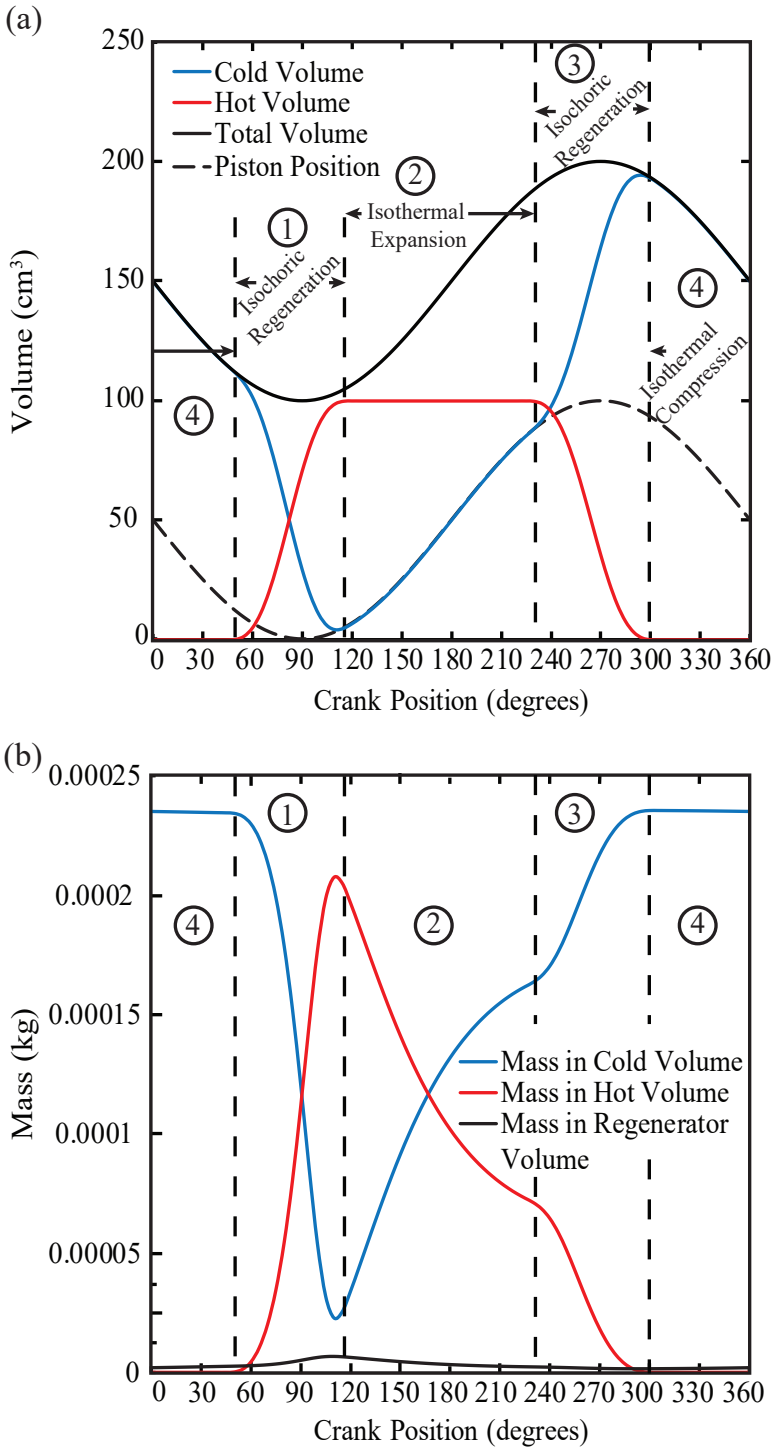

Figure 16. (a) Volume and (b) mass of the cam driven displacer and sinusoidal piston as a function of crank angle (θ).

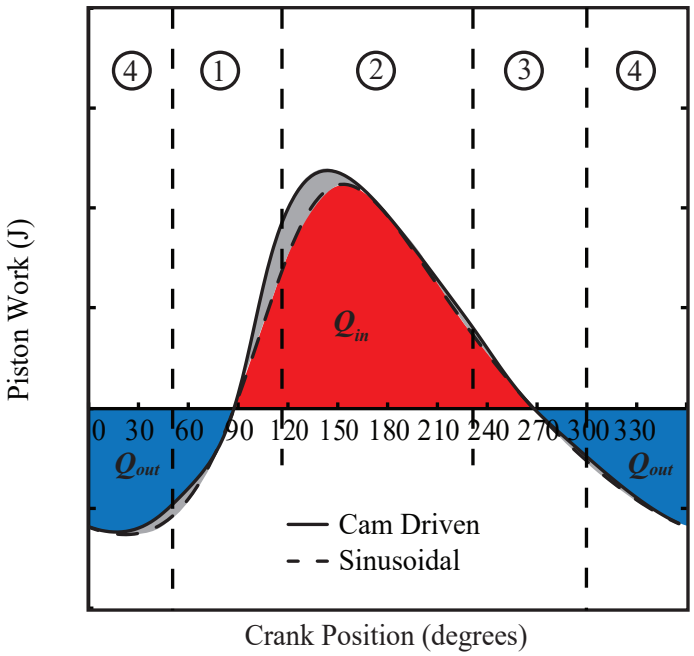

Figure 17. Piston work versus crank angle (θ) for the cam-imposed variant and full sinusoidal beta-type Stirling engine. The W_{out} corresponds to Q_{in} and is shown as red, and the W_{in} corresponds to Q_{out} and is shown as blue. The gray shading shows the advantage that the cam driven cycle has over the full sinusoidal cycle.

the hybrid arrangement nets a beneficial gain both during expansion and compression stages of the cycle. This effect can be seen in Figure 17.

Figure 17 shows the piston work for the sinusoidal engine described in the previous section with an overlay of the cam driven displacer Stirling engine. Due to the non-sinusoidal motion of the displacer the modified Stirling engine is able to compress and expand more effectively. Because the displacer dwells with the hot volume near zero, the compression portion of the cycle is able to happen with less work required. This is because the mass is isolated on the cold side of the engine for the majority of the duration of the compression keeping the specific volume, v, low making compression easier to achieve. This is shown by the gray shaded region beside the blue Q_{out} and blue potion of the graph. Similarly, during expansion the displacer dwells with its respective cold volume

near zero, the expansion portion of the cycle is able to happen more effectively and produce more work. This is because the mass is more isolated on the hot side of the engine for the majority of the duration of the expansion, keeping the specific volume, v, as high as possible increasing the maximum attainable work. This is shown by the gray shaded region beside the blue Q_{in} and red potion of the graph. With the ability to dwell the displacer, this arrangement is able to more easily compress and more effectively expand, and the total net work and efficiency is increased. The net work and efficiency quantities of both the cam driven variant and the full sinusoidal Stirling engine are shown in Table 3.

By applying Equations (2.12)-(2.14), and (2.18), and adapting them to apply to the volumetric variations of the cam-driven displacer of the beta/gamma configuration with a cold volume and hot volume according to Equations (3.5) and (3.4), and using the values listed in Table 1, the thermal efficiency was found to be 43.8%, which is a reduction of 17.6% from the Carnot efficiency. Similar to the alpha, beta and gamma-type engines, the efficiency varies with temperature ratio, so the resulting efficiency is plotted for a range of temperature ratios in Figure 18. Within the typical operating range described above, the effects of the cam and crank operation on beta/gamma Stirling engines results

Table 3. Work and efficiency values for comparing the cam driven displacer to the full sinusoidal Stirling engine.

Process	**Cam Driven**	**Sinusoidal**	**Delta**
Work Out (J)	25.3	23.0	2.3
Work In (J)	-14.2	-14.8	0.6
Net work (J)	11.1	8.2	2.8
Efficiency ($\eta, \%$)	43.8	35.8	8.0
Power Factor	$\left(W_{Net_{\mathrm{Cam,d}}}/W_{Net_{\mathrm{Sin}}}\right)$	1.35	
Efficiency Factor	$\left(\eta_{\mathrm{Cam,d}}/\eta_{\mathrm{Sin}}\right)$	1.22	

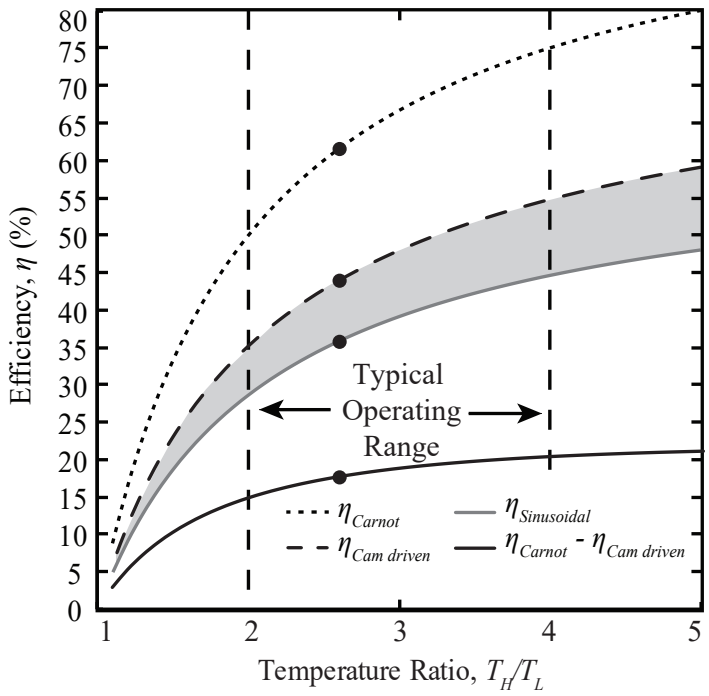

Figure 18. Efficiencies for Carnot, the cam driven cycle, and the sinusoidal cycle for a beta and gamma-type Stirling engines at various temperature ratios. The point indicates the values corresponding to the engine details provided in Table 1.

in a reduction from Carnot thermal efficiencies ranging from 14.8% to 20.3%, as seen in Figure 18. To further conceptualize the hybrid Stirling engine efficiency and net work increases, power factor and efficiency factor are calculated to contrast the improvement over the pure sinusoidal variant. These values indicate a 35% increase in net work and a 22% increase in efficiency, that the hybrid cam design has over the pure sinusoidal engine.

The findings demonstrate that the efficiency from the sinusoidal motion of the standard configuration can be increased if pure sinusoidal movement is enhanced by adopting motion that better follows the thermodynamic principals of the ideal Stirling cycle. This is demonstrated with a plausible modification to the beta/gamma-type engines by utilizing a cam to drive the displacer to move when the piston is approaching the top and bottom locations as well as dwell during key parts of the compression and expansion

processes. The cam-driven displacer modification is able to increase the efficiency of the standard beta and gamma-type configurations by 6.5% to 10%, when operating within typical operating temperature ratios. Further modifications, involving both the piston and displacer operating with non-sinusoidal motion, may have potential to push the efficiency values even closer to Carnot. By having a power piston mechanism that is able to transfer torque effectively, while also deviating from sinusoidal movement, may help to recover additional efficiency and net work losses beyond the half cam and half sinusoidal arrangement presented.

Chapter 4

Conclusions

A comprehensive discretized model of an alpha-type Stirling engine was developed to investigate the thermodynamic deviations resulting from sinusoidal operation. The deviation of the sinusoidal cycle from the ideal cycle results in a reduction in the attainable net work and thermal efficiency. A generalized engine is analyzed and found that due to the sinusoidal motion, the alpha-type Stirling engine was only able to produce 65.9% of the ideal work. The resulting thermal efficiency was 34.4%, which corresponded to a reduction of 27.1% from the maximum attainable Carnot efficiency. Within typical operating temperature ratios of 2 to 4, the reduction in thermal efficiencies ranged from 23.6% to 29.5% respectively. For the case that was investigated in present analysis also revealed that a phase angle of 60° corresponded to the largest attainable thermal efficiency, with a value of 36.4%. For beta and gamma-type Stirling engines, the thermal efficiency was found to be 35.8%, which corresponded to a reduction of 25.7% from the maximum attainable Carnot efficiency. Similar to the alpha-type engine, within the typical operating temperature ratios of 2 to 4, the reduction in thermal efficiencies ranged

from 21.4% to 30.4% respectively. It has been shown that sinusoidal operation impacts alpha, beta, and gamma Stirling configurations in a similarly adverse manner.

The finding of a substantial reduction in efficiency versus the theoretical efficiency helps to explain why practical Stirling engines built with sinusoidal motion have low efficiency values. To begin improvements on the thermodynamic operation of the Stirling cycle, an augmented Stirling configuration is presented and can be implemented into beta and gamma-type Stirling geometries. The new design utilizes cam geometry to operate the displacer to better follow the ideal Stirling cycle. Within similar constrains to the previous studies it was found that 8% of the 25.7% that is lost due to pure sinusoidal motion can be recuperated. The typical temperature ratios of 2 to 4 produce efficiency values of 35.2% to 54.7% respectively. In comparison between the cam driven displacer with a sinusoidal piston engine to the pure sinusoidal engine a power increase of 35% and a efficiency increase of 22% is obtained.

4.1 Recommendations

The following points are the next steps for future works to better understand and improve Stirling engine technology. These recommendations are beyond the scope of this thesis but can serve as important steps for future investigation:

- In order to substantially increase Stirling engine operation, the motion of the engine components eg. the piston(s) and displacer need to deviate from pure sinusoidal motion in accordance to the ideal cycle.

- Additional methods for deviating from sinusoidal movement that can be implemented into a Stirling engine should be investigated, including; inventive linkages, cams, and other mechanical and electro-mechanical couplings.

- Designers need to be aware of the dynamics of deviating from sinusoidal movement and that noise needs to be minimized for sustainable operation.

- Future models and analysis that can account for, and model, advantageous volumetric variations should then incorporate heat transfer and fluid flow equations to further increase the accuracy and predict experimental losses that will inevitably accompany the system.

- Produce an experimental prototype to test non-sinusoidal designs to validate this and future models.

Bibliography

[1] Y. Cengel and M. Boles. *Thermodynamics: An engineering approach, 8th ed.* New York: McGraw-Hill Education, 2015.

[2] Microgen Engine Corporation. "Engines". `http://www.microgen-engine.com/products/engines/`. Accessed: 2018-09-11.

[3] J. Egas and D. M. Clucas. Stirling engine configuration selection. *Energies*, 11(3), 2018.

[4] W. R. Martini. *Stirling engine design manual*. US Department of Energy, Office of Conservation and Solar Applications, Division of Transportation Energy Conservation, 1978.

[5] K. Mahkamov. Design improvements to a biomass stirling engine using mathematical analysis and 3d cfd modeling. *Journal of Energy Resources Technology*, 128(3):203–215, 2006.

[6] A. Ross. *Stirling cycle engines*. Solar Engines, 1981.

[7] F. Wu, L. Chen, C. Wu, and F. Sun. Optimum performance of irreversible Stirling engine with imperfect regeneration. *Energy Convers. Manage.*, 39(8):727–732, 1998.

[8] S. Isshiki, A. Sakano, I. Ushiyama, and N. Isshiki. Studies on flow resistance and heat transfer of regenerator wire meshes of Stirling engine in oscillatory flow. *JSME Int J., Ser. B*, 40(2):281–289, 1997.

[9] B. Kongtragool and S. Wongwises. Thermodynamic analysis of a Stirling engine including dead volumes of hot space, cold space and regenerator. *Renew. Energy*, 31(3):345–359, 2006.

[10] M. Briggs. *Improving free-piston Stirling engine power density.* PhD thesis, Case Western Reserve University, 2015.

[11] G. Schmidt. The theory of Lehmann's calorimetric machine. *Z. Ver. Dtsch. Ing.*, 15(1), 1871.

[12] T. Finkelstein. Generalized thermodynamic analysis of Stirling engines. Technical report, SAE Technical Paper, 1960.

[13] G. Walker. An optimization of the principal design parameters of Stirling cycle machines. *J Mech Eng Sci*, 4(3):226–240, 1962.

[14] D. Kirkley. Determination of the optimum configuration for a Stirling engine. *J. Mech. Eng. Sci.*, 4(3):204–212, 1962.

[15] I. Urieli and D. M. Berchowitz. *Stirling cycle engine analysis.* Taylor & Francis, 1984.

[16] R. Dyson, S. Wilson, and R. Tew. Review of computational stirling analysis methods. In *2nd International Energy Conversion Engineering Conference*, page 5582, 2004.

[17] T. Finkelstein. Optimization of phase angle and volume ratio for stirling engines. Technical report, SAE Technical Paper, 1960.

[18] T. Finkelstein. A new isothermal theory for stirling machine analysis and a volume optimization using the concept of 'ancillary'and 'tidal'domains. *Proceedings of the Institution of Mechanical Engineers, Part C: Journal of Mechanical Engineering Science*, 212(3):225–236, 1998.

[19] L. B. Erbay and H. Yavuz. Analysis of the stirling heat engine at maximum power conditions. *Energy*, 22(7):645–650, 1997.

[20] M. Costea, S. Petrescu, and C. Harman. The effect of irreversibilities on solar stirling engine cycle performance. *Energy conversion and management*, 40(15-16):1723–1731, 1999.

[21] F. Formosa and G. Despesse. Analytical model for Stirling cycle machine design. *Energy Convers. Manage.*, 51(10):1855–1863, 2010.

[22] C.-H. Cheng and H.-S. Yang. Optimization of geometrical parameters for stirling engines based on theoretical analysis. *Appl. Energy*, 92:395–405, 2012.

[23] M. H. Ahmadi, A. H. Mohammadi, S. Dehghani, and M. A. Barranco-Jimenez. Multi-objective thermodynamic-based optimization of output power of solar dish-stirling engine by implementing an evolutionary algorithm. *Energy conversion and Management*, 75:438–445, 2013.

[24] F. Formosa and L. G. Fréchette. Scaling laws for free piston stirling engine design: Benefits and challenges of miniaturization. *Energy*, 57:796–808, 2013.

[25] K. K. Makhkamov and D. Ingham. Analysis of the working process and mechanical losses in a stirling engine for a solar power unit. *Journal of solar energy engineering*, 121(2):121–127, 1999.

[26] C. Cinar. Thermodynamic analysis of an α-type Stirling engine with variable phase angle. *Proc. Inst. Mech. Eng. Pt. C J. Mech. Eng. Sci.*, 221(8):949–954, 2007.

[27] C.-H. Cheng and Y.-J. Yu. Dynamic simulation of a beta-type Stirling engine with cam-drive mechanism via the combination of the thermodynamic and dynamic models. *Renew. Energy*, 36(2):714–725, 2011.

[28] M. Campos, J. Vargas, and J. Ordonez. Thermodynamic optimization of a stirling engine. *Energy*, 44(1):902–910, 2012.

[29] J. Bert, D. Chrenko, T. Sophy, L. Le Moyne, and F. Sirot. Simulation, experimental validation and kinematic optimization of a stirling engine using air and helium. *Energy*, 78:701–712, 2014.

[30] S. Alfarawi, R. Al-Dadah, and S. Mahmoud. Influence of phase angle and dead volume on gamma-type stirling engine power using CFD simulation. *Energy Convers. Manage.*, 124:130–140, 2016.

[31] S. Ranieri, G. Prado, and B. MacDonald. Efficiency reduction in stirling engines resulting from sinusoidal motion. *Energies*, 11(11):2887, 2018.

[32] K. J. Waldron, G. L. Kinzel, and S. K. Agrawal. *Kinematics, dynamics, and design of machinery*. John Wiley & Sons, 2016.